

# Master's thesis

**NTNU**  
Norwegian University of Science and Technology  
Faculty of Information Technology and Electrical  
Engineering  
Department of Engineering Cybernetics

Tore Mattias Apeland

## Design of Solar Measurement IoT Node Using LPWAN

Master's thesis in MTTK  
Supervisor: Geir Mathisen  
October 2019



Norwegian University of  
Science and Technology



Tore Mattias Apeland

# Design of Solar Measurement IoT Node Using LPWAN

Master's thesis in MTTK  
Supervisor: Geir Mathisen  
October 2019

Norwegian University of Science and Technology  
Faculty of Information Technology and Electrical Engineering  
Department of Engineering Cybernetics



Norwegian University of  
Science and Technology



---

# Summary

In this project, we want to develop an embedded platform based on the low power wide area network technologies LoRa and NB-IoT, that is capable of reporting the potential solar energy production to a central server. Restricting the size and cost of the equipment is also a design goal.

A set of system requirements is proposed, and a design approach is presented. The required functionality of the device is divided into modules, and a selection of components and a general schematic is presented for two different designs. One design is based on the nRF9160 NB-IoT and LTE-M enabled microcontroller, while the other uses a RN2483 LoRa modem with a ATtiny817 as central unit.

A solar harvester circuit with a rechargeable battery is suggested for power management. Although the basic features of the module was functioning, it was discovered that the selected solar panel was not large enough to power the system during the dark winter season, thus, a larger panel should be used.

For finding the potential solar panel production, a sensor for measuring the short circuit current and the temperature of the solar panel was made. Together with the characteristics of the panel, the solar irradiance can be estimated, which in turn describes the possible production from the panel. Sensors for the orientation and position of the device was also added to provide additional information about the observed irradiance.

A model for the device software, communication protocol, and message structure was proposed, and a test sending and receiving messages from a server using MQTT was successfully performed.

The work presented in this project falls short of a full implementation, but it can serve as a basis for finalizing the design of the sensor node.

---

# Sammendrag

I denne oppgaven ønsker vi å utvikle en embedded plattform basert på lavenergi nettverksteknologiene LoRa og NB-IoT. Enheten skal være i stand til å rapportere potensiell solenergiproduksjon til en sentral server. Det er også et designmål å begrense utstyrets størrelse og kostnad.

En liste med systemkrav foreslås, og et overordnet design blir utviklet. Enhetens funksjonalitet deles inn i moduler, og et utvalg av komponenter samt en generell skjemategning presenteres for to ulike design. Det ene designet er basert på nRF9160 mikrokontrolleren med NB-IoT og LTE-M funksjonalitet. I det andre designet brukes et RN2483 LoRa-modem sammen med en ATTiny817 som styringsenhet.

En energihøster krets for sollys med et oppladbart batteri legges frem som en løsning på strømforsyning. Modulen ble verifisert som fungerende, men det kom frem at det valgte solpanelet ikke var stort nok til å kunne skaffe tilstrekkelig energi i vintermørket. Derfor burde et større panel benyttes.

For å finne den potensielle solcellepanelproduksjonen ble det laget en sensor for å måle kortslutningsstrømmen og temperaturen til solcellepanelet. Sammen med panelets egenskaper kan sollysets innstrålingstetthet estimeres. Ut fra dette kan man finne den mulige produksjonen til panelet. Sensorer for å bestemme enhetens orientering og posisjon ble lagt til for å gi ytterligere informasjon om den observerte irradiansen.

En modell for oppbygningen av enhetens programvare, kommunikasjonsprotokoll og meldingsstruktur ble foreslått. Det ble gjennomført en test hvor enheten lykkes i å sende og motta meldinger fra serveren med bruk av MQTT.

Arbeidet som presenteres i dette prosjektet er ikke en komplett implementasjon, men fungerer som et grunnlag for å ferdigstille sensornoden.

---

# Preface

This project was done as the final part of my Master's study in 'Cybernetics and Robotics' at the Norwegian University of Science and Technology.

I would like to thank my supervisor, Geir Mathisen, for the guidance and continuous support he provided during this work. Moreover, I would like to thank the student organization Omega Verksted for providing the equipment and software necessary for soldering and PCB design. Finally, I would like to thank Nordic Semiconductor for providing free development boards for the nRF9160 SiP.

I received a three week extension of time for this project, moving the deadline from 23.09.19 to 14.10.19.



# Contents

<b>Summary</b>	<b>i</b>
<b>Preface</b>	<b>iii</b>
<b>Table of Contents</b>	<b>vi</b>
<b>List of Tables</b>	<b>vii</b>
<b>List of Figures</b>	<b>x</b>
<b>Abbreviations</b>	<b>xi</b>
<b>1 Introduction</b>	<b>1</b>
1.1 Background . . . . .	1
1.2 Motivation . . . . .	2
1.3 Objective and Scope . . . . .	2
1.4 Outline . . . . .	2
<b>2 Literature Review</b>	<b>3</b>
2.1 Instrumentation for Environmental Monitoring . . . . .	3
2.1.1 Applications . . . . .	4
2.1.2 Sensor Nodes . . . . .	5
2.2 Communication Methods . . . . .	6
2.2.1 Link layer, Physical Mediums and its Reach . . . . .	7
2.2.2 Internet layer . . . . .	12
2.2.3 Transport layer . . . . .	13
2.2.4 Application layer . . . . .	13
2.3 Self-powered IoT Solutions . . . . .	15
2.3.1 Energy Harvesting . . . . .	15
2.3.2 Batteries . . . . .	17
2.4 Snow Avalanche Detection Using a Geophone Sensor Network . . . . .	18

---

2.5	Project Sunroof . . . . .	18
2.6	Summary of Literature Study . . . . .	19
<b>3</b>	<b>System Requirements and Design</b>	<b>21</b>
3.1	System Requirements . . . . .	21
3.2	Overall System Design . . . . .	22
3.2.1	Power Module . . . . .	23
3.2.2	Communication Module . . . . .	25
3.2.3	Controller Module . . . . .	26
3.2.4	Sensor Module . . . . .	28
3.2.5	Networking . . . . .	30
<b>4</b>	<b>Implementation</b>	<b>33</b>
4.1	Sensor Node Hardware . . . . .	33
4.1.1	Main Components . . . . .	35
4.1.2	Closed Circuit Current Measurement . . . . .	41
4.1.3	Power Module . . . . .	44
4.1.4	PCB Design . . . . .	51
4.2	Software . . . . .	55
4.2.1	Sensor Node Firmware . . . . .	55
<b>5</b>	<b>Results &amp; Discussion</b>	<b>61</b>
<b>6</b>	<b>Conclusion</b>	<b>65</b>
<b>7</b>	<b>Future Work</b>	<b>67</b>
	<b>Bibliography</b>	<b>69</b>

# List of Tables

2.1	Frequencies and usages [14] [47]	7
2.2	Overhead to payload ratio.	13
4.1	MAX44284 variants. Assumed $V_{dd} = 3.3V$	43
4.2	Resistor values for battery charge mangement programming	47



# List of Figures

2.1	Weather station in Sølendet nature reserve [41] . . . . .	5
2.2	Geophone system in Sanneslia, Nordland [23]. . . . .	19
3.1	Sensor node context diagram. . . . .	22
3.2	Overall system functionality. . . . .	23
3.3	Overall system design . . . . .	24
3.4	Cellular network coverage map for Telenor [5] . . . . .	26
3.5	Cellular IoT network coverage map for Telia.[6] . . . . .	27
3.6	Map of LoRa basestation locations that are registered at "The Things Network". There are 113 of these gateways in Norway. [24]	27
4.1	Proposed system structure. . . . .	34
4.2	Main components overview for nrf9160 based design. Product images are from mikroe.com, no.mouser.com, ti.com, and nordicsemi.com. . . . .	35
4.3	Main components overview for ATtiny817 based design. Product images are from mikroe.com, no.mouser.com, ti.com, quectel.com, and microchip.com. . . . .	36
4.4	A visualization of what a finalized implementation might look like. . . . .	37
4.5	Typical application of the DS3231 real time counter, as suggested by its datasheet [3]. . . . .	37
4.6	Digital thermometer DS18B20 attached to the backside of the solar panel using thermal paste and kapton tape. . . . .	39
4.7	Wiring schematic for the NB-IoT design. . . . .	40
4.8	Wiring schematic for the LoRa design. . . . .	41
4.9	Typical application circuit for MAX44284 [9]. . . . .	42
4.10	Schematic for the current sense circuit. $R1 = 0.62\Omega$ . . . . .	44
4.11	Simplified illustration of BQ25505 application. . . . .	45
4.12	Schematic for a solar harvesting circuit based on BQ25505. . . . .	46
4.13	Schematic for DC-DC converter based on TPS61200. . . . .	49
4.14	Power module circuit schematic. . . . .	50

---

4.15	Power module circuit layout.	51
4.16	Power module PCB that was used for testing.	52
4.17	Power module circuit schematic.	52
4.18	PV current sensor PCB.	53
4.19	Layout reference for BQ25505 [33]	53
4.20	Layout reference for BQ25505 [32]	54
4.21	Simplified model of the proposed sensor node mainloop.	55
4.22	Model of the proposed sensor node mainloop.	56
4.23	A screenshot of the ThingsBoard dashboard, showing the received GPS position of the device.	59
5.1	Power-voltage curve of the Mikroe-SW0.4M solar panel.	62
5.2	DC-DC module test.	63

---

# Abbreviations

ADC	=	Analog to Digital Converter
GPS	=	Global Positioning System
IC	=	Integrated Circuit
IMU	=	Inertial Measurement Unit
JSON	=	JavaScript Object Notation
LED	=	Light-emitting Diode
MPPT	=	Maximum Power Point Tracking
PCB	=	Printed Circuit Board
PV	=	Photovoltaic
RTC	=	Real-time Counter
SiP	=	System-in-Package
SoC	=	System on a Chip
TWI	=	Two Wire Interface
UART	=	Universal Asynchronous Receiver/Transmitter



# Introduction

## 1.1 Background

The Internet of Things, or internet connected embedded devices, is an expanding topic, where more and more devices are made to interface with cloud based solutions. In line with this, new methods are developed to meet the energy and connectivity needs of smaller devices. The topic of this project is to explore some of the already available technologies and components that can be applied to make a remote embedded platform. In particular, low power wide area network communication and energy harvesting is highlighted.

Further, the use of solar energy harvesting at home has become more popular of late. Often, an estimate of the available solar power is given in advance of installment. This is typically found using satellite imagery and weather data [16]. It could be interesting to develop a small device for performing in-field prospecting of the solar potential at a given location.

There exists a number of devices already capable of this, such as weather stations and home projects. However, these are sometimes large installments, rely on short range communication such as WiFi, or use older communication technology as for example old 2G cellular modems. For this project, we want to look at the development of an affordable and flexible sensor node, with low maintenance and long range capabilities.

The suggested implementation presented in this project serves as a basis for finalizing the design of a self powered sensor node, with the ability to report the potential production from a solar panel.

## 1.2 Motivation

One of the main motivations for this project is to explore the possible solutions for the instrumentation of the device. Especially, the LPWAN technologies LoRa and NB-IoT and the new LTE modem nRF9160 from Nordic Semiconductor are of interest. Further, being able to monitor the potential production of a solar panel can be useful for determining good locations for solar panel installments. In addition, it might be possible to use the data collected by multiple nodes to generate a prediction of what the production of other nearby solar panels will be in the near future.

## 1.3 Objective and Scope

The main goal of this project is to make a prototype for the embedded platform. However, the implementation presented only lays out the foundation for which a design for the sensor node can be completed.

The following list describes the main objectives of this project

- Study instrumentation for remote low power embedded systems
- Define the system requirements
- Design a functional model, and propose an overall schematic for the device
- Suggest a strategy for device firmware and communication protocols
- Create a prototype of the device

## 1.4 Outline

First, in chapter 2, a literature review is conducted. Here, the basics of existing solutions regarding environmental monitoring, wireless communication, and energy harvesting are explored. Next, in chapter 3 a set of requirements is presented for the system, and possible design solutions are examined based on what was found in the literature review. It is argued that the device should rely on solar energy harvesting, and that the solar potential would be measured using the short circuit current and temperature of the solar panel.

Further, in chapter 4, a model of the embedded node is presented, where the functionality of the device is divided into modules. A set of components and a schematic describing the wiring of the modules is also shown. Two different propositions are made, one based on NB-IoT and one using a LoRa modem. In addition, a plan for the device software is introduced.

Chapter 5 presents the results of the project and suggests potential improvements to the design. Finally, chapter 6 and 7 provides a conclusion and suggestions for further work.

# Chapter 2

## Literature Review

Three of the main challenges in this project involve the instrumentation, the communication, and the self powering of IoT solutions. This chapter explores some existing technologies within these fields, that could be applicable for this project.

### 2.1 Instrumentation for Environmental Monitoring

In general, environmental monitoring involves collecting sensor data in order to assess the status of an environment. In this case, the term environment is given in the broad sense as in the surroundings of a location, and can refer to enclosed spaces such as the indoor area of a factory, or larger locations such as a city. There are a great many environmental variables that can be monitored.

#### Commonly Monitored Environmental Parameters

- Air quality
  - Gaseous pollutants such as ozone, carbon monoxide, sulfur dioxide, lead, nitrogen oxides, carbon dioxide, chlorofluorocarbons
  - Particulate matter such as PM<sub>10</sub>, PM<sub>2.5</sub>. Particles small enough to be drawn deep into the lungs of a human.
- Weather parameters
  - Air pressure
  - Temperature
  - Humidity
  - Rainfall

- Wind speed and direction
- Lighting conditions
- Water quality [12]
  - Physical characteristics such as temperature, colour, contained sediments
  - Chemical characteristics such as dissolved oxygen, acidity , salinity, nutrients
  - Biological characteristics such as bacteria and algae
- Radiation

### 2.1.1 Applications

Environmental monitoring is applied in different situations for varying purposes. For example, in the case of monitoring the environment of a factory building, one could be interested in sampling air and temperature parameters to confirm the environment is suitable for human workers. Being able to detect hazardous matters and high temperatures emitted from factory machinery can be used both as a warning system and as regulation information for systems that have an impact on the environment.

A different example is weather stations, that are known for their provision of atmospheric measurement data, needed for generating weather forecasts. Moreover, some weather stations are used for assessing the human impact on the natural environment, that normally features specialized sensors for measuring pollutants. Figure 2.1 shows an example of a remote automatic weather station, located in Sølendet nature reserve.



**Figure 2.1:** Weather station in Sølendet nature reserve [41]

## 2.1.2 Sensor Nodes

Instrumentation for environmental monitoring encompasses many kinds of systems, but as of late small sensor nodes have been gaining popularity. These kind of nodes are usually associated with being inexpensive and small in size, in addition to featuring wireless connectivity and low power consumption. Due to their low cost they are widely available for both commercial and industrial practices. There exists many tutorials and open source software solutions directed towards hobby electronics [1].

### Sensor Node Components

It's typical for such sensor nodes to include one or more simple sensors, a low power microcontroller, a battery, and a separate module for communication purposes. Of course, this may vary as some units are less remote installations with access to wired power or communication bus. Many remote low-maintenance devices also feature an energy harvester in order to replenish the battery. Furthermore, the capabilities and limitations of a node is governed by the selection of components.

For example, some platforms are designed to use Wi-Fi communication as opposed to connecting to a cellular network, and will only work in the vicinity of Wi-Fi routers. On the other hand, using a cellular network with a SIM card will most likely be more expensive, and also require more power to drive the radio circuit. Hence, one might prioritize the Wi-Fi communication method if the environment allows it. In general, it is important to

define the technical requirements of a node before selecting its components.

Which parameters are of interest is dependent on the intended use of the system, and requires knowledge of the environment that is to be monitored. In order to obtain robust data from the monitoring system, the data collection strategies and methods of analysis should be well defined. Hence, choosing the right sensor and sampling method for the environment and fully understanding the surroundings effect on the sensor is an essential part of the system design.

### Sensor Data Sampling

Sensor nodes usually has a strict power budget due to often depending on energy scavenging and small batteries for system power. In order to minimize power consumption, electrical on-board components can be powered down or put into sleep mode, resuming operation only when needed. Hence, deciding an interval between sampling sessions and the number of samples per wake-up is an important part of the design. The system should choose the sampling rate based on the dynamics of the parameter being monitored in order to give a realistic depiction of the signal.

Another aspect to consider is the rate of distribution of sampled data. The communication module tends to be among the most power consuming components. Thus, some implementations choose to limit transmission to short intervals in order to conserve energy. In regard to this, data can be processed and compressed for the sake of lessening the amount of information that is to be sent. For example, transmitting an average of the last ten measurements rather than all of them.

The downside of limiting sampling and sending time is that it introduces additional delay, in addition to providing a sparser set of measurements. Hence, the system will be less suited for real-time applications, but the overall energy needed can be lower.

## 2.2 Communication Methods

Sensor systems are often required to relay collected information to other physical devices, in order to process and monitor the data. There are many configurations to choose from when designing the communication part of a system, however, the more beneficial options can only be identified based on the system needs.

The Internet of Things sets out to connect physical things such as sensors to the internet. In order to communicate on the internet a common protocol stack is required. Depending on the type of connection used, it is sometimes needed that the IoT device implements the necessary communication stack itself. This is best explained using the TCP/IP reference model, which divides the different part of the internet into a application, transport, internet,

and link layer [35] [34].

### 2.2.1 Link layer, Physical Mediums and its Reach

When selecting a link technology, the capacity of the communications link should be capable of supporting the needed throughput. Moreover, a highly influential factor is the available infrastructure, that will govern the possibility of wired power and communication, and the coverage of wireless networks. The available power also restricts the kind of radio technology that can be used. Also, the physical size of the system will affect what kind of hardware that can be fitted, as some antennas might be too large.

#### Spectrum used in wireless networks

In wireless technology radio waves are most commonly used as the signal carrier. Radio waves are part of the electromagnetic spectrum, and range from about 30Hz to 300GHz. The choice of frequency greatly affects the range of the signal, where in general low frequencies can diffract around larger obstacles and will reach further. However, higher frequency signals are able to provide a higher data rate, hence, there is a need to balance fast transfers and long range properties. This is one reason why there is a diverse selection of radio technologies that focuses on varying range and transfer speed. Table 2.1 shows a few technologies and their associated frequencies. Note that the table does not list all possible frequencies for each entry.

**Table 2.1:** Frequencies and usages [14] [47]

Freq. Band	Typical Frequency		Usage
LF	148.5 - 283.5	kHz	Longrange radio broadcast
	125	kHz	Low Frequency RFID
MF	526.5 - 1606.5	kHz	AM radio
VHF	87.5 - 108	MHz	FM radio
UHF	430 - 440	MHz	LDP433, LoRa
	470 - 790	MHz	TV broadcast
	868	MHz	LPWAN (LoRa, Sigfox)
	1452 - 1492	MHz	DAB-radio
	1.8	GHz	Mobile GSM, 4G (LTE)
	1559 - 1610	MHz	GPS
	2.1	GHz	Mobile UTMS
SHF	2.4	GHz	Wi-Fi, Bluetooth, ZigBee, ANT
	2.6	GHz	Mobile 4G (LTE)
	3.5	GHz	Mobile 5G
	5	GHz	Wi-Fi

### **Radio Frequency Management**

Extremely high frequencies that well exceeds the radio waves part of the electromagnetic spectrum are generally not viable as carrier waves, due to lack of equipment and wave propagation properties. This implies that radio waves is a limited resource. There exists regulations for radio communication systems and frequency usages that are governed by a few large institutions on an international level, some of them are listed below.

Nkom Nasjonal Kommunikasjonsmyndighet - Regulates telecommunications in Norway

FCC Federal Communications Commission - Regulates telecommunications in USA

ETSI European Telecommunications Standards Institute - Leading standardization organization for Information and Communication Technology standards, with global influence.

ERO European Radiocommunications Office - Headquarters in Denmark. Distribution point for all ECC documentation.

CEPT European Conference of Postal and Telecommunications Administrations - Regulates telecommunications in Europe, and has three committees: CERP, ECC, Com-ITU.

In Norway, Nasjonal kommunikasjonsmyndighet (Nkom) is responsible for regulation of telecommunication, and they have selected to regulate frequencies in the range 8.3 kHz - 3000 GHz [14]. Devices operating outside this range are still required not to interfere with other communication, and have restrictions regarding signal field strength.

When designing a radio based solution it is important to be aware of regulations. The process of prototyping and receiving approval for an antenna circuit can be time consuming, which is why projects often will benefit from using existing designs and components.

### **Wide Area Networks**

Wide area networks (WAN) are networks that extends large geographical areas. The cellular networks are examples of WANs, where radio masts are distributed to provide wide coverage. Devices can connect to the network using a relatively small antenna and modem, and provides a way for embedded devices to reach the internet.

The 2G (GSM), 3G (UMTS), 4G/LTE networks are commonly used by battery powered solutions in order to relay information. These networks are often mentioned in conjunction with mobile phones, but are also applied in other embedded systems. However, a downside of these networks is that sending traffic requires a SIM card with a paid subscription. Below is a list of some of the key features of 2G, 3G, and 4G/LTE networks.

- **Cost:** Modems are widely available and relatively inexpensive, although components that are compatible with newer networks tends to cost more. An example is the SIM800 module for 2G networks, which is priced at about 4.5\$ [2]. The cost of a SIM card subscription is dependent on the local supplier and the amount of traffic from the device.
- **Coverage:** The cellular networks generally have good coverage, even in remote locations. In Norway, the 2G network has the best coverage, and is available most places [5] [6].

- **Data Rates:**

2G	220 kbit/s
3G	42 Mbit/s
4G/LTE	100 Mbit/s

- **Power Consumption:** The power consumption of a modem is highly dependent on the quality of the implementation and mode of operation, but a demand of several hundred mA when the radio is powered is probable. Especially some of the older modules, such as the SIM800, are not low-power friendly.
- **Development:** In Norway, the 3G network is in the process of being shut down, and will be gone by the end of the year 2019 [27]. What will become of the 2G network is unclear, as it still supports many older modems that is incompatible with 4G. Furthermore, the 4G/LTE network is still being expanded and improved on, making it credible that 4G will also be available in the near future.

### Low Power Wide Area Networks

The demand for low-energy communication have been steadily increasing, which has prompted the development of low power wide area networks (LPWAN). These networks usually features long-range communication with low data rates, and are directed towards IoT devices.

Narrow Band Internet of Things (NB-IoT/Cat-NB1) and LTE Cat-M1 (LTE-M) are LPWAN that uses the 4G infrastructure. Hence, they provide a low power alternative to other mobile networks, while also offering similar coverage. However, this technology is relatively new and is not necessarily available in all countries.

LTE-M is different from NB-IoT as it is optimized for higher bandwidth and mobile connections, and is designed to provide for medium throughput applications. It is based on LTE technology but uses a narrower band than general LTE, which gives it longer range but lower throughput. Moreover, it can be used for moving applications that will operate over multiple regions.

NB-IoT does not directly use the regular LTE physical layer, but is designed to operate in and around LTE bands. Not all existing LTE base stations support NB-IoT technology,

and requires an equipment upgrade in order to provide coverage. Furthermore, it uses a much smaller bandwidth than LTE-M, which again gives it longer range but less throughput. In contrast to LTE-M, the technology is not suited for roaming applications [8]. The list below shows some of the NB-IoT and LTE-M common key features.

- **Cost:** Modems cost about the same as for other cellular networks. For example the NB-IoT and LTE-M capable nRF9160 chip is priced at 25\$ [2]. SIM card subscriptions are available cheaper than for regular 4G/LTE, however the intended data usage per time is much lower. Telenor, a Norwegian telecommunications company, offers NB-IoT for 99 Kr per year (about 10\$) with 5 MB of data [7] per year, which amounts to about 13.7 kB per day.
- **Coverage:** Provides similar coverage to 4G in Norway, as it connects through the same infrastructure. Although, the use of a smaller bandwidth gives the technologies longer range.

- **Data Rates:**

NB-IoT	60 kbit/s
LTE-M	375 kbit/s (HD-FDD), 1 Mbit/s (FDD)

- **Power Consumption:** It can be challenging to give an accurate estimation of the power consumed by low power modems, as it is dependent on usage. Looking at the nRF9160, the modem can demand currents ranging from 45 to 380 mA based on required signal strength.
- **Development:** The development of NB-IoT and LTE-M is backed by large telecommunication companies and is being expanded alongside the improvements for 4G networks. Thus, it seems plausible that the technology will have coverage in the near future.

### Non-cellular LPWANs

LoRa (Long Range), Sigfox, Ingenu, and Weightless are examples of LPWAN directed towards IoT devices that does not rely on the proprietary cellular network infrastructure. Instead, custom base stations, also referred to as gateways, are mainly used. These base stations can sometimes be purchased and operated by both public network operators and individuals.

LoRa and Sigfox are often compared as they both use the open ISM bands. In Europe the common frequency is 868 MHz. In terms of differences, Sigfox is mainly for uplink communication and has very low data rate, in addition to a small message capacity. Hence, it is mostly suited for simple devices that transmit infrequently. Moreover, the Sigfox company manages and deploys all base stations, and base their business model mostly on selling the network as a service.

On the other hand, LoRa has an open network standard which means that other hardware manufacturers can design modules and gateways that conforms with LoRa specifications.

There also exists multiple network protocols that is based on LoRa radios, namely LoRaWAN and Symphony Link. The former is the standard for LoRa networks that uses messages with small payloads, while the latter was made later in response to the weak points of LoRaWAN. Furthermore, LoRa networks has a symmetric link such that devices can both send and receive messages.

Ingenu uses open ISM bands and operates at 2.4 GHz, which is a significantly higher frequency than LoRa and Sigfox. This is reflected by the transfer rates and ranges offered by Ingenu, as it has shorter range but better throughput. However, this network mainly resides in some areas of USA, and similarly to Sigfox uses proprietary base stations.

Weightless is a set of several technology standards for LPWAN communication. Firstly, Weightless-W is an open standard that operates in the TV broadcast spectrum by utilizing whitespace, e.g. currently unused frequencies. Secondly, Weightless-N and Weightless-P are protocols that operates on the sub-gigahertz unlicensed spectrum. Weightless-N provides an uplink service similar to that of Sigfox, except at higher speeds and shorter range. Weightless-P is for bidirectional communication.

- **Cost:** Sigfox has some of the cheapest radio modules that goes for about 5\$, while LoRa modems starts at about 10\$ [2]. Modules for Ingenu and Weightless are less available.
- **Coverage:** Sigfox is mostly available in France and surrounding countries. Most of LoRa base stations are found in urban areas, but there is no guarantee that any given city will have a network available. However, new base stations can be installed by third parties. In Norway, Sigfox is unavailable, but LoRa can be found in any major city.

- **Data Rates:**

Sigfox	100 bit/s upload and about 1.6kB budget per day
LoRaWAN	300 bit/s - 50 kbit/s depending on channel bandwidth
Weightless-P	200 bit/s - 100 kbit/s
Ingenu	624 kbit/s upload, 156 kbit/s download

- **Power Consumption:** Sigfox and LoRa uses a very narrow bandwidth, and may in general be more low power than NB-IoT.
- **Development:** LPWAN is a shifting market where the future of present technologies are unknown. Hence, it is possible that devices developed for currently relevant LPWAN will be outdated in the near future.

## Local Area Networks

Local Area Networks (LAN) are, as the name suggests, more localized networks than WANs. Many modern LAN technologies use the 2.4 GHz ISM band, and are optimized for

throughput rather than range compared to WANs. Since the maximum distance between sender and receiver is shorter in LANs the required radio effect is much lower than for WAN technologies. Below is a list of some well known LAN technologies.

- Wi-Fi
- Bluetooth
- Bluetooth Low Energy
- ANT
- ZigBee

Even though LAN technology allows for lower power applications, the obvious drawback is the range of the signal. In general, outdoor applications cannot rely on having access to LAN networks. The list below shows the main outline of LAN technology.

- **Cost:** The cost of radio modems are dependent on the target network and technology, but in general, modules for common technologies such as Wi-Fi or Bluetooth are inexpensive. For example, the Wi-Fi module ESP8266 is available for about 1\$ [2].
- **Coverage:** Usually, coverage must be provided by a locally owned base station, such as a Wi-Fi router or a smartphone with Bluetooth. Hence, LAN applications are more situation specific and might be less suited for generic remote devices.
- **Data Rates:** LAN technology has very good throughput, but it depends on the implementation used. For instance, a standard Wi-Fi network can normally provide several hundred Mbit/s, while Bluetooth Low Energy (BLE) has a few kbit/s depending on the link configuration.
- **Power Consumption:** The antennas required for LAN technology can require very little energy, due to short distances. As an example, the nRF51 BLE device can use as little as 34  $\mu$ A when using infrequent advertising and processing.
- **Development:** LAN technologies are being improved and updated frequently. Especially, devices using commonplace networks such as Wi-Fi might have a better chance of being compatible with future revisions of base stations.

## 2.2.2 Internet layer

At the internet level of the TCP/IP model, the Internet Protocol(IP) is used. It provides communication capabilities such as addressing and signaling, which is essential to identify and route information through interconnected networks. In IPv4, the address is represented by 32 bits while in IPv6 the address space is represented using 128 bits[44][37]. Currently the addressing space for IPv4 is near depleted. Thus, IPv6 with its larger address space is said to be a crucial enabler for IoT adoption to grow. Other possibilities such as network address translation may help prolong the IPv4 usability, but this breaks the end-to-end

connectivity, and make the system dependent on third party network nodes.

Currently the minimum IPv4 header size is 20 bytes and the minimum IPv6 header is 40 bytes. For both standards the header size may grow depending on whether optional functionality or signaling is used.

### 2.2.3 Transport layer

Transmission Control Protocol (TCP) is one of the main transport protocols, which is implemented on top of IP in the transport layer. Its main purpose is to provide a reliable connection with error checks and flow control, for delivery of IP datagrams [45]. When establishing a TCP connection, it utilizes 3 IP packets, 3 more are used to close the connection. The TCP minimum header size is 20 bytes.

User Datagram Protocol (UDP) is the other major transport protocol in the TCP/IP transport layer. Contrary to TCP, it makes no effort to verify that the IP datagram was received. UDP is thus said to be a connectionless transport protocol. This allows UDP to use less data than TCP. UDP uses a minimum header size of 8 bytes [46].

The overhead of using transport protocols and internet protocols depends both on the amount of data being sent and the protocols used. Moreover, the protocols used for the link layer, which lies under both the transport and internet layer, can also introduce additional overhead. For example, ethernet has a header of 18 bytes. The maximum segment size denotes how much information can be packet into a datagram, typically this is about 1560 bytes. Table 2.2 shows a comparison of overhead to payload ratio.

**Table 2.2:** Overhead to payload ratio.

MIX	Protocol/header bytes	1 byte data	500 byte data	1500 byte data
UDP/IPv4	8+20 bytes	28:1	7:125	7:375
UDP/IPv6	8+40 bytes	48:1	12:125	4:125
TCP/IPv4	(20+20)*6 bytes	240:1	12:25	4:25
TCP/IPv6	(20+40)*6 bytes	360:1	18:25	6:25

### 2.2.4 Application layer

There is often a need to collect and store data transmitted from remote devices on a server. Data stored on a server is easily accessible, and can be used for backups, computations, and data visualisation. For the device data to reach a server, it must traverse the internet using the Internet Protocol (IP). In many cases, the underlying layers is handled by the operating system or support libraries, allowing the developer to focus on the application layer, i.e. the messaging protocol.

An example of an application layer protocol is HTTP, which is known best for its usage with websites. Although this protocol is often used with IoT devices, it is not optimized for the needs of low power applications. Below is a list of some features that are often desired for IoT applications.

- Sending information from one to many
- Event triggers
- Transporting information over unreliable networks
- Sensitivity to data volume and power consumption
- Responsiveness (near-realtime delivery)
- Scalability
- Security

There are several alternatives to HTTP that focuses on light weight solutions for IoT device communication, the following list shows a few of them.

MQTT	Message Queuing Telemetry Transport is an open source lightweight message based protocol, that implements a publish/subscribe model. It is made with machine to machine (M2M) in mind, and provides a lossless bidirectional link using TCP/IP. It is popular in IoT systems due to its small footprint[11].
CoAP	Constrained Application Protocol is closely related to HTTP, but focuses on low overhead in packages and can handle communications over lossy connections. The protocol was designed to be translatable to HTTP, hence, it is useful for interfacing with web servers.[48]
AMQP	Advanced Message Queueing Protocol is a message oriented middleware, that features message orienting, reliability, security, queuing, and routing. The protocol is not as lightweight as MQTT, but features more advanced options.[15]

To some degree IoT specific messaging protocols have moved away from traditional request-reply where clients and server communicate directly, over to a publish subscribe model where messages are published to a broker and consumed by subscribers [38]. This model has several benefits over the traditional request-reply model, as it allows publishers to not know who or how many subscribers are consuming their messages, and messages are exchanged in an asynchronous fashion. In other words, it allows published messages to be retained at a broker for later consumption by any set of subscribers [43].

Some IoT messaging protocols, such as MQTT, further enables a decoupling of session state and connection state, thus avoiding costly application session and state synchronization, should a connection be broken due to unreliable network conditions or IoT nodes entering power saving sleep states.

## 2.3 Self-powered IoT Solutions

Self-powered embedded solutions are able to harness energy from the environment in order to power itself. This ability is often required for low-maintenance or remote applications, as they might operate in areas without grid power or ease of access. Also, changing the battery for a system that contains several hundred nodes is unwanted work.

### 2.3.1 Energy Harvesting

In order to obtain reliable energy harvesting, information about the environment is needed. Not all sources of energy are always available, in addition, some energy sources will be more easily exploitable.

Mainly, it is possible to split the types of environments into two variants, namely controlled and uncontrolled [36]. A controlled environment refers to artificial environments where variables such as lighting and temperature can be controlled, i.e. indoor areas. Environments where there are no apparatus to influence conditions are referred to as uncontrollable environments, and is typically found at outdoor locations.

Many of the same harvesting techniques can be applied both for controlled and uncontrolled environments, but the source of the energy is usually more reliable in the case of a controlled environment. For example, PV panels will usually be powered by sunlight outdoors, while indoor environments can either use artificial lighting or a directed laser.

#### Light

Light is perhaps the most commonly used source for energy harvesting, which is due to being predictable and often present. The energy from light can be harvested using PV panels, which are found in many devices, e.g. calculators, ticket machines, and wristwatches.

PV panels comes in varying sizes and implementations, which dictates the properties of the panel. Normally, for IoT applications monocrystalline or polycrystalline panels are used, due to their balance of cost and quality. In general, the monocrystalline panels are slightly more expensive but offers greater efficiency [36].

Furthermore, PV panels requires impedance matching to function the most efficiently. The voltage of a PV panel will decline as for low impedance loads. The technique Maximum Power Point Tracking (MPPT) is often used to find the optimal combination of current draw and voltage in terms of power. Commonly, the technique is implemented using a specialized integrated circuit (IC) that is part of the energy harvesting circuit.

As an alternative to PV panels, photosynthesis can be used as a part of a biological or electrochemical reaction in order to generate energy. This technology is still novel and

under development.

In controlled environments, energy can be injected by installing artificial lighting, or by the use of a directed laser.

## **Thermal Energy**

Thermoelectric and pyroelectric generators are used to scavenge energy from heat. In summary, thermoelectric devices exploits heat gradients, while pyroelectric devices benefits from heat fluctuations [36]. In controlled environments, heat radiated from machines and other equipment can be used as a source for energy for both technologies. However, in uncontrolled environments significant temperature gradients are not very common, and usually heat fluctuations have a low frequency. Hence, thermal energy scavenging is less seen applied in uncontrolled environments.

Moreover, radioisotopes can be used as a heat source, and is used in several space crafts. This is generally not suited for IoT applications, due to its harmful nature.

## **Kinetic Energy**

Kinetic energy can be scavenged from the environment by using equipment that capture vibrations and the movement of fluids [36]. A classic example is a turbine, that can harvest power from air flows or water streams. A typical turbine might be too large in size to be considered using for IoT applications, however there exists micro turbines that are directed towards smaller installations.

Furthermore, vibrations can be harvested for energy using piezoelectrics or mechanical vibration harvesters. Piezoelectrics harvesters accumulates charge when subjected to mechanical stress, usually from bending or impacts, while mechanical vibration harvesters usually involve translating vibrations to electrical energy using induction.

Moreover, vibration energy can be scavenged using electrostatic and triboelectric harvesters. The former is based on utilizing the charge made from the motion between two materials, while the latter depends on the charge generated by bringing together and separating materials.

Another technique is to harvest energy from the variation of atmospheric pressure or the expansion and contraction of liquids due to temperature fluctuations. This is often done using bellows or a similar mechanism.

### Electromagnetic Energy

Magnetic induction can be used for wireless energy transfers, and depends on using a direct magnetic coupling between two coils. This technology is found in items such as electric toothbrushes and smartphones, and serves as a way to charge the device. Similarly, radio waves can be used for RF induction. However, magnetic induction is more suited for short distance larger power transfers, while radio frequency harvesters are able to function over longer distances but with less power [36].

Both these technologies are dependent on energy sources that are mostly present in controlled environments, although RF signals are often found in uncontrolled environments as well.

### 2.3.2 Batteries

Batteries are able to create electric charge from chemical reactions, and serve as a portable power source. There are multiple types of batteries that use different chemicals with varying properties. Perhaps most notably some batteries can be recharged, while others are designed to be used once and thrown away when depleted.

When designing a low maintenance IoT device, rechargeable batteries can be used in conjunction with energy harvesters in order to supply a reliable power source. This is useful when the harvested energy sources are not always available, such as with sunlight, where PV panels can struggle to scavenge enough energy after sundown. In these cases, excess energy harvested during daytime can be stored in a battery to cover the nightly power needs of the system.

#### Li-Ion & Li-Po

A popular choice of rechargeable batteries are lithium-ion (Li-Ion) or lithium-polymer (Li-Po) batteries. These types of batteries have little memory effect, i.e. the loss of charge capacity due to being partially discharged, and is known to be low maintenance. Li-Ion differs from Li-Po in the choice of chemical electrolyte, as Li-Po uses a solid or gel like electrolyte instead of a liquid.

Li-Ion batteries have the advantage of having high energy density and can provide high currents. However, they are volatile and require safety circuitry to prevent the battery cells from being over- or undercharged. Li-Po batteries are a safer alternative to Li-Ion batteries, although these also require special attention when charging [29]. They also weigh less, suffer less from aging, and retain their charging capacity for longer. The downsides of Li-Po are lower energy density and capacity, and they also usually have a higher production cost.

### **Supercapacitors**

As an alternative to batteries supercapacitors are sometimes used. One of the main advantages of supercapacitors is that the number of recharge cycles is much higher, hence they have a longer lifespan. Furthermore, supercapacitors has a wider temperature operating range, and might not lose performance to the same degree as batteries would at certain temperatures. On the other hand, supercapacitors have less energy density than Li-Ion and Li-Po batteries, and the self-discharge is somewhat higher than that of an electrochemical battery. Moreover, there is a gradual voltage loss that will decline in correspondence to current flow, hence supercapacitors does not provide the same steady voltage as batteries could.

## **2.4 Snow Avalanche Detection Using a Geophone Sensor Network**

During the winter of 2017/2018 the Norwegian Public Roads Administration added two new snow avalanche detection system, one situated in Nordland and one in Telemark. The system is used to detect snow avalanches in a hillside above a car road. Upon detection, the system can close off the road using traffic lights, and dispatch a warning message in the form of an E-mail [23].

The system consists of groups of geophones that are spread out in the hillside, where each of the sensor groups has a corresponding radio mast. The radio masts form a wireless mesh network that allows all masts to relay messages to a base station. Furthermore, each mast features an a microcontroller, a radio module, a battery, and a solar harvester.

More specifically, the 32-bit microcontroller EFM32 is used to collect and analyze the output of multiple geophones. The processed geophone data is then transmitted by a LPT5902-IPM radio module. This IC implements a transport protocol for reliably relaying messages using a self-healing mesh network operating in the 2.4GHz band. Multiple PV panels are installed in order to supply a 6V 70mA output, which is fed to a MCP73811 IC that manages the charging of lithium-ion batteries. [19]

Messages are ultimately received at a gateway at the base of the hillside. From there, they are sent to servers using both a wired connection and a 3G/GPRS link [18].

## **2.5 Project Sunroof**

Project Sunroof [16] is an initiative started by Google that attempts to estimate the production of PV panels on rooftops in urban areas in the USA. As an alternative to field measurements, calculations are based on geographical data. More specifically, aerial imagery and is used to generate a 3D model of rooftops and nearby obstacles. This model can

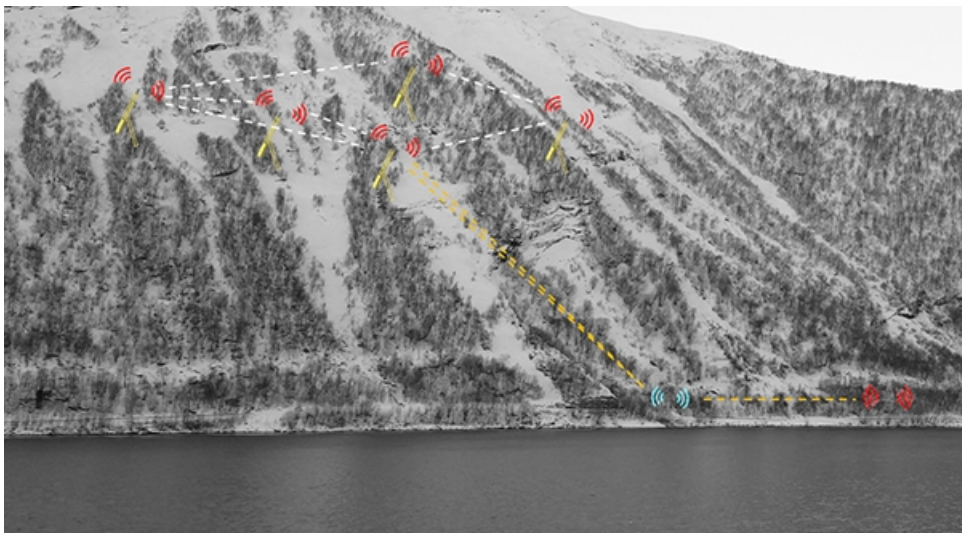


**Figure 2.2:** Geophone system in Sanneslia, Nordland [23].

then be employed to study the shadows cast on the roof as the sun changes position. Then, in conjunction with weather statistics, an estimate can be given for PV panel production.

This method depends purely on geographical information, and uses a deep learning network to identify rooftops. Hence, an estimate can effectively be given for large areas based on existing data sets, without the need to deploy physical sensors. However, estimations can suffer from errors generated by the deep learning network or from outdated imagery data. Moreover, factors such as light obstructing particle matter or the reflectivity of the surroundings are not necessarily captured by the geographical data.

## 2.6 Summary of Literature Study

Through this study it has become clear that there are many different technologies for wireless communication and energy harvesting. For low power systems that only needs to send a small amount of data, LAN technology should be used if possible. However, if range is required, an LPWAN modem can provide several kilometers of range, and in general has lower power consumption than other long range radio technology. From the selection of LPWAN, not all are available in Norway, which must be considered before choosing the modem.

From the different types of energy sources, sunlight is the most predictable energy source in most cases. Monocrystalline panels are often more expensive than polycrystalline panels, but offers a higher level of efficiency. For storing the energy, a Li-Po battery should be used for low power systems, although Li-Ion batteries can be cheaper.

The snow avalanche detection system is an example of kind of sensor node we are looking to develop. However, this system is based on a sensor network and depends on other nodes to successfully relay data. For our application, it is desired that each node can be deployed separately.

Project Sunroof excels at wide scale estimation for solar panel production. This differs from the sensor node based approach, which will be able detect ongoing trends closer to real time.

# Chapter 3

# System Requirements and Design

In this chapter the intended functionality of the system is described, and a design is suggested. Section 3.1 presents the system requirements, while section 3.2 suggests a general design and discusses some of the possible solutions.

## 3.1 System Requirements

The goal is to design an embedded sensor platform that can be used to investigate the potential energy production of a PV panel at a given location. Data collected by the device is to be centralized at a server for further use. Moreover, the system should be easily scalable to monitor several locations, and each node should be composed of relatively inexpensive components.

The sensor platform is directed towards outdoor use. This implies that the device should not rely on wired power or communication. In this project, the LPWAN technologies LoRa and NB-IoT are the main focus. These communication methods are not directed towards roaming applications, which is why only stationary designs will be considered. Moreover, the system should be low maintenance, and is to be functional over longer periods of time. Also, the platform must be small in size and portable, such that it can be easily fastened to structures. Figure 3.1 shows the context diagram for the sensor node.

The list below summarizes the desired specifications for the sensor node.

1. Wirelessly connected at outdoor locations with at least 2km range
2. Measure potential output production for a PV panel
3. Has a clock for tagging data with time of collection, where the clock should not drift more than 10 seconds per day.

4. The intervals for data sampling and transmission of sensor data must be remotely configurable, with a maximum send interval of 1 minute.
5. Must be able to provide geographical location data on request
6. Small in size, no larger than an A4 sheet of paper
7. Easily scalable, in the sense that adding more instances of sensor nodes requires little work
8. Self-powered
9. Affordable
10. Sensor node lifetime of minimum 2 years

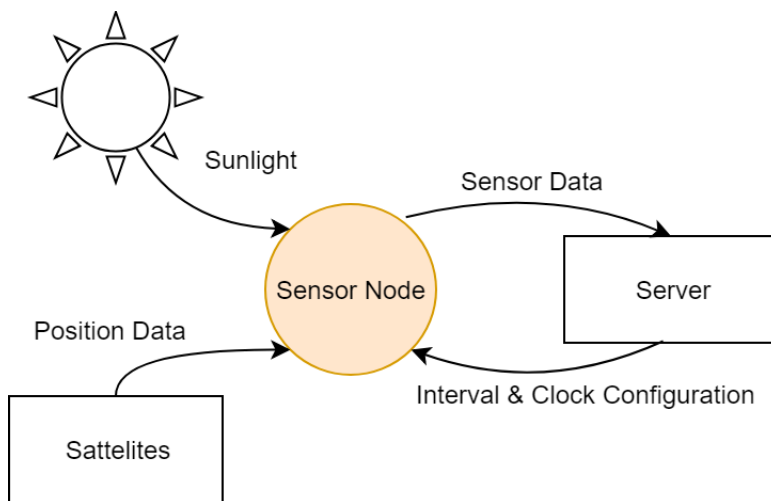


**Figure 3.1:** Sensor node context diagram.

## 3.2 Overall System Design

Based on the specifications in section 3.1, a suggestion for the general system structure is shown in figure 3.3. The figure has of two main parts: the sensor node and the internet connected server. The sensor node consists of four modules, namely controller, sensor, communication, and power module.

Firstly, the controller module is the core component that governs the other modules. Some of its main tasks are keeping track of time, sleep cycles, communication parameters, and gathering sensor data. Hence, it is suggested that the module has a way of processing and storing data, as well as a method for accurately keeping track of time. Secondly, the

sensor module contains the mechanism for obtaining a reading of the PV panels currently available production. Moreover, one might consider including a sensor for finding the orientation of the physical device, as such information could be useful when evaluating PV panel efficiency.

Next, the communication module provides the method of communication, and must be able to relay messages to the internet. Furthermore, the module is also responsible for obtaining the position of the device. Finally, the power module should deliver a steady voltage supply to the other system modules, and uses energy harvesting to replenish its resources.

On the other side of the wireless communication link we have the server. Its only requirements are to accept incoming connections, and to send configuration settings back to the sensor node. However, the design should include a front end user interface to make it easier to view and verify data. For this, a quick solution is desired, i.e. an existing software solution should be used rather than writing a framework from scratch. Figure 3.2 shows the general intended functionality of the system.

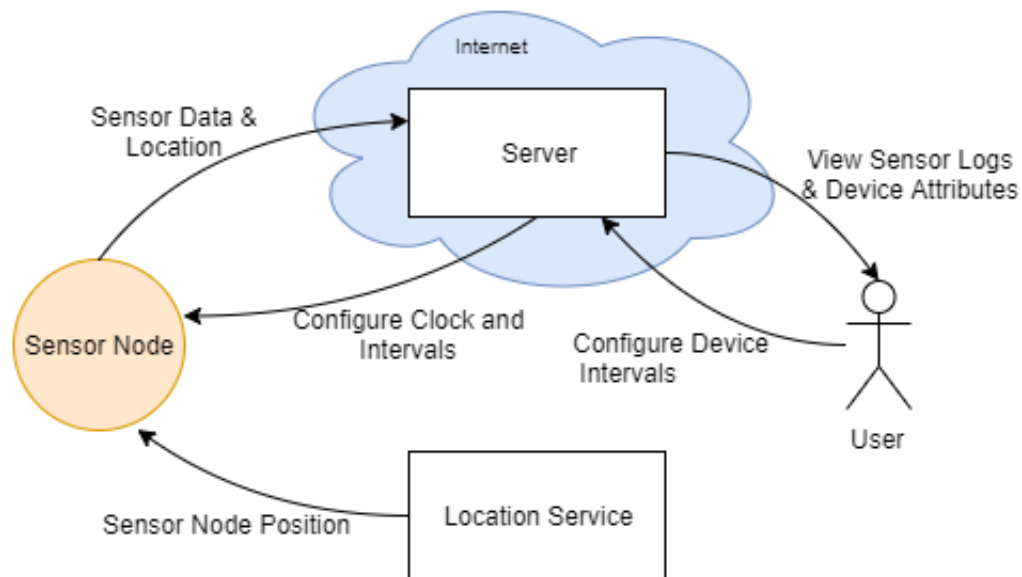


**Figure 3.2:** Overall system functionality.

### 3.2.1 Power Module

The power module is responsible for supplying a steady voltage supply to the other modules. The system is required to function autonomously over longer periods of time, without access

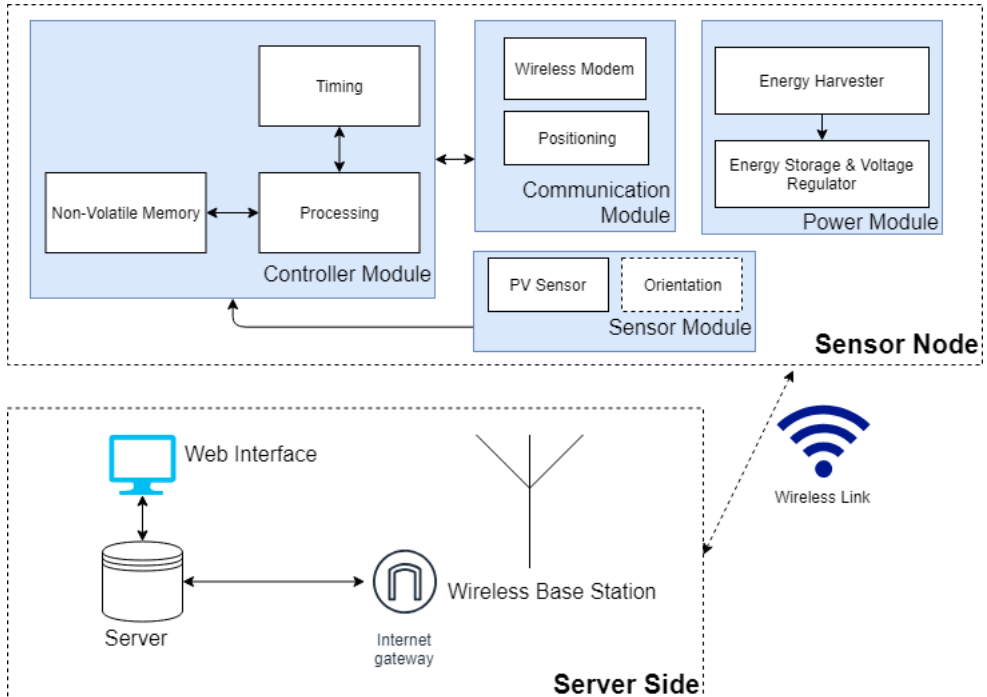


Figure 3.3: Overall system design

to an external power connection. Relying solely on a battery might prove challenging due to the energy optimization needed. Having a small energy budget also puts a great restrictions on the frequency of transmissions. Hence, energy harvesting should be part of the power module.

From the selection of different energy sources, sunlight might be the most predictable alternative. Additionally, components for harvesting sunlight are common, well documented, and relatively inexpensive. Options to sunlight are wind or rain power. However, the degree of presence of these weather elements are highly dependent on the geographic location, and might be unreliable as a source for daily energy harvesting. Also, micro turbines are in general more costly than PV panels.

If the system is to function in the absence of a scavengable energy source, a method for storing energy is also needed. A Li-Po battery together with a charge managing IC can be used for energy storage. As mentioned in section 2.3.2, Li-Po technology generally has less aging effect and better temperature operating range than Li-Ion batteries, but has lower energy density and can not provide as high currents. In this case, longevity is preferred over performance, as the current drain of a low-power IoT system is expected to be modest compared to the battery's capabilities.

Supercapacitors can also be used for energy storage, and generally offers a much higher number of recharge cycles. Yet, they have a smaller energy density than Li-Po batteries, and also self-discharge at a higher rate. Hence, using supercapacitors might depend on more frequent exposure to sunlight. Combining both supercapacitors and batteries might provide a way to extend the power module lifetime, while also maintaining good energy storage capabilities. However, this will complicate the design.

Furthermore, the battery output should be regulated to provide a stable system power line at the correct voltage. For this a DC-DC converter could be used. The type of DC-DC converter is dependent on the battery voltage and the target system voltage, as different scenarios would require either a buck or boost converter, or both. LDO regulators on the other hand are cheaper in production, but have poor efficiency compared to DC-DC converters, which is an unwanted property in this system.

### 3.2.2 Communication Module

As stated in the system requirements, the communications module must be able to connect from outdoor locations at over longer distances, which means this application can not easily rely on LAN technology such as Wi-Fi. In addition, the system depends on an internal power supply, which means that minimizing the current consumption is of high priority. Thus, as described in section 2.2.1, LPWAN based technology is suited for this task.

From the selection of LPWANs NB-IoT is a good candidate. To begin, NB-IoT is a cellular network that shares base stations with 4G infrastructure, providing coverage in large parts of Norway, the exception mostly being uninhabited areas. Compared to LTE-M, NB-IoT is directed towards simpler applications that are static and send very little data. NB-IoT has a lower subscription cost as well as longer range. In this regard, it is the better option between the two if the number of bytes sent per year is low enough.

Another interesting candidate is LoRa, from the category of non-cellular networks. Its main advantages are a small power consumption, cheap modems, long range, and the absence of a subscription fee. However, the network requires its own type of base stations, that are mainly only found in major cities. The figures 3.4 and 3.5 shows the coverage of cellular networks, while figure 3.6 is a map of LoRaWAN gateways registered at "The Things Network" company. Although not all of Norway's LoRa gateways are included, it is clear that the cellular networks provides much better coverage in total. Other LPWAN technologies such as Sigfox, Ingenu and Weightless are generally less attractive than LoRa due to the lack of gateways or availability of hardware.

An important property required by the network module is the ability to enter a power saving mode when not in use. Sending messages using wireless communication will most likely be the most energy costly operation of the system. Energy can be saved by sending data only a few times each day. If the system was to be closer to a real-time application, the size of batteries and energy harvesters would have to be increased to meet the required

current consumption.

Moreover, the location of the sensor node is necessary to correctly tag the sampled data. The most straightforward solution to this is the use of a GPS module in order to obtain the device coordinates. Some communication modules, especially the cellular based modems, will include a GPS feature without any extra cost. Having a GPS module in addition the communications module can be costly for the power budget of the system. As an alternative, since the device is designed to be static, the coordinates of the sensor node can be registered upon deployment using a separate GPS device. In other words, in an attempt to save components and energy, the position can hard-coded into the controller module's firmware or be manually paired with the device on the server. However, this solution could prove inconvenient and introduces more complexity to the system.

Another important aspect of the communication is the protocols used and the packaging of data, which is the topic of section 3.2.5.

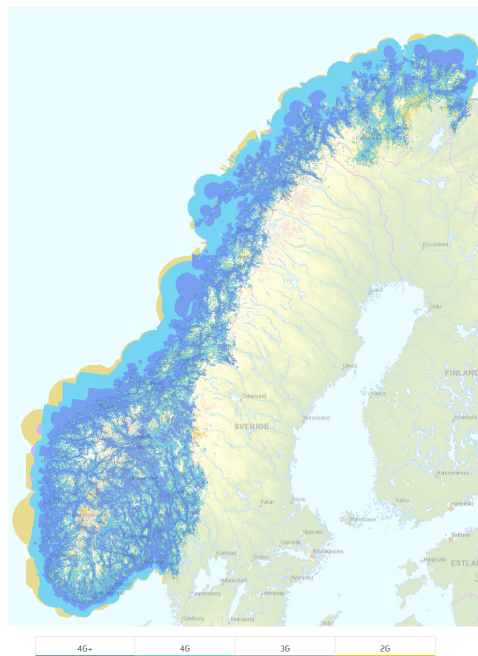


**Figure 3.4:** Cellular network coverage map for Telenor [5]

### 3.2.3 Controller Module

The controller module is responsible for reading and processing the sensor output, as well as operating the communications module in order to send the data to the server. This suggests



**Figure 3.5:** Cellular IoT network coverage map for Telia.[6]

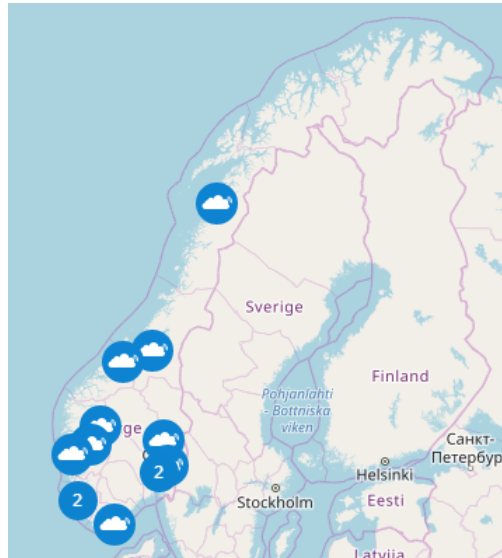


**Figure 3.6:** Map of LoRa basestation locations that are registered at "The Things Network". There are 113 of these gateways in Norway. [24]

that a microcontroller should be part of the module, and it needs to have the necessary features for interfacing with the other components. For example, an ADC or SPI interface might be needed to obtain sensor data. Considering that sunlight has relatively slow dynamics, it is likely that very frequent sampling is not needed, although this depends on the type

of sensor. If in addition the amount of data to send is small, a very fast microcontroller is superfluous.

Furthermore, sampled data from sensors can be processed on the embedded platform in order to provide more accurate readings, as well as reducing the amount of bytes to send. For example, when reading analogue values the system can take multiple rapid samples and use the average value as the result, with the purpose of reducing the effect of transients in samples. Also, averaging data in general reduces the amount of samples that the platform needs to send to the server. Which data is sent from the sensor node is also of importance. For instance, the embedded platform can combine different sensor output in order to produce a single measurement of PV panel efficiency, or it can send sensor output as separate values and leave it to the server to process it. The latter is a more flexible solution as it makes it possible to later change how the data is processed, in addition to giving better insight into the dynamics that led to the results. However, the drawback is that more data is relayed, which taxes both the communication link and system power.

Another concern is the buffering of unsent data. The microcontroller should have access to non-volatile memory in order to prevent the loss of samples in the event of power outage. Not all microcontrollers support writing to the internal flash during runtime, such that an external memory component might be needed. Flash memory is commonly used, and there exists implementations with a small standby current consumption and simple serial interface. Usually the current drain will scale with the size of the memory, hence, the choice of memory capacity should be decided by the desired buffer time in regard to sample data size and frequency. For instance, given 500 kB of flash memory, 32 bit of sample data with 32 bit of timestamp overhead, and a sampling interval of 10 seconds, the system would be able to retain approximately a week worth of data.

The control module also needs a system clock, and a way to synchronize this using the wireless link or GPS. Some embedded systems would use an RTC to keep track of time passed, which is commonly implemented using a 32.768 kHz quartz crystal. Microcontrollers will sometimes have an internal RTC. However, it might be worth keeping an external clock module separate with its own backup battery, such that the counting does not stop during power outage. RTCs are usually very low power and can operate on a coin cell battery for years.

### 3.2.4 Sensor Module

The sensor module must provide an instrument that allows finding an estimate of the energy production of a PV panel. There are several approaches to this. Firstly, it is possible to study the amount of sunlight that reaches the device, and give an estimate based on this. Not all frequencies of electromagnetic radiation is useful for a PV panel, as lower frequency waves lack the energy to generate a current, although this depends on the materials used in the panel. A different method is to monitor the output of a PV panel. Then, later compare its properties to other panels, and use the sampled data to give an estimate.

A pyranometer can be used to measure the solar irradiance on a surface, also known as watt per square metre, and are designed to capture radiation in a range somewhere between 300 nm and 3000 nm [25]. Some implementations of pyranometers are thermopile devices, and are based on measuring heat from sunlight. There are also silicon based photovoltaic pyranometers which feature photodiodes. A thermopile pyranometer can absorb waves from most of the solar radiation, while the photovoltaic systems have a spectral range usually somewhere from 350 nm to 1120 nm. For this project, using a photovoltaic pyranometer could be a possible solution, as they exists in small sizes with low power consumption, and they have a spectral response similar to PV panels. However, a professional pyranometer can be a costly component, for example the smaller photovoltaic pyranometers SP-110-SS and SP-212-SS from Apogee starts at about 3000 NOK [20].

An alternative to pyranometers is to directly measure the production of a solar panel. One approach is to connect the PV panel to a solar harvester circuit that embeds the MPPT algorithm, which attempts to maximise the effect that is being extracted from the panel. The current and voltage from the panel can then be measured to observe the current power production. However, this method necessitate that the MPPT circuit is always active, which might not be the case if the energy reserves are full. Also, the accuracy of the MPPT also becomes a factor of the measurements. Instead, measuring the short circuit current of the panel will give a measurement that is a function of the sunlight that hits the panel and temperature, as shown in equation 3.1 [39].

$$Irradiance_{PV}^{PVRD} = \frac{I_{sc,M}}{1 + \alpha_{Isc} * (T_{cell} - T_{ref})} * \frac{G_{ref}}{I_{sc,ref}} \quad (3.1)$$

In equation 3.1  $I_{sc,M}$  is the measured short circuit current of the PV device,  $\alpha_{Isc}$  is the temperature coefficient of  $I_{sc,M}$ . Further,  $T_{cell}$  is the cell temperature of the solar panel,  $T_{ref}$  is the reference calibration temperature.  $G_{ref}$  is the reference calibration irradiance of the PV device,  $I_{sc,ref}$  is the reference short circuit current. These values are either listed in the PV device datasheet or found by calibration.

A downside with these methods is that the characteristics of the panel must be known in order to be able to make comparisons to other panels. Also, the temperature of the panel effects its efficiency, short circuit current, and open circuit voltage. Hence, a temperature sensor should be included to monitor the PV panel. Aside from this, it allows the re-use of an already included component, rather than having a separate component for light detection.

In regard to measuring PV panel output, ADCs are commonly used. When measuring output voltage, the maximum panel voltage tends exceed the limits of a typical microcontroller ADC. In these cases a voltage divider circuit can be applied to reduce the range of the voltage. Next, when measuring currents, a shunt resistor, a low resistance precision resistor, can be placed in series with the rest of the circuit. When current passes through, there will be a small voltage drop across the resistor. This voltage can also be measured using an ADC, although the signal is usually boosted using a operational amplifier or similar. Since the value of the resistor is known, the voltage can be translated to current using Ohm's law.

Finally, it could be interesting to know the orientation of the device. This could be useful additional information when interpreting the PV potential sensor data. The energy production of a PV panel is affected by the angle that sunrays hit the panel, where ideally the sun is normal to the PV panel surface [16]. In order to capture the orientation of the device the sensor module must include sensors for finding rotation and cardinal directions. Finding the rotation can be done by adding a 3-axis accelerometer. As for the cardinal directions, a magnetometer is suitable.

Both of these sensors exist as a low profile ICs with no moving parts. Yet, as the system is static, embedding orientation sensors might be seen as a waste of resources. Instead, one might consider installing the equipment in a predetermined position upon deployment, although this would require separate instruments. It's also worth noting that sensors such as magnetometers are dependent on proper calibration to function accurately.

### 3.2.5 Networking

Compared to a sensor node, a server has an incredible availability of computing power, energy, and memory. For this reason, the networking aspect of the system should be designed in favor of the sensor nodes. To begin, the choice of protocol governs the total amount of data needed to send a payload between devices. Keeping the bytes sent to a minimum is crucial both for energy saving and in regard to a data budget. As mentioned in section 2.2.4, there are application layer protocols that specialize in lightweight IoT communication. For this project, MQTT might be a feasible choice, as it has only 2 bytes of overhead in the application layer, payload acknowledgment, and supports binary data. In addition, there exists free open source implementations of MQTT brokers that can be built and run on most server machines.

From the list of system requirements it is clear that the device needs a way to perform two-way communication. The sensor node needs to send sensor data to the server, and the server must be able to relay attributes such as polling and sending intervals. In the case of a MQTT protocol, the publish and subscribe system must be used. Hence, the sensor node can publish data to one topic, and subscribe to another for settings information. It's essential that each sensor node has its own individual topic to subscribe to, such that a message directed to a single node is not received by other nodes, as it would be a waste of data. Moreover, incoming messages to the server can be distinguished by adding an identifier unique to the node to either the payload, topic, or username of the MQTT session.

Further, there is the question of the message formatting. A simple approach would be to send information using JSON encoding, as this format is easy to handle. However, JSON is a text based format which excels at compatibility and ease of use rather than compact data representations. In other words, packaging messages using a binary format would reduce the amount of bytes sent. However, binary formats are less flexible, and requires the sender and receiver to completely agree upon a message structure.

Depending on the intended use of the platform, reporting information a few times a day could be sufficient when the interest lies with the long term statistics. In addition, reporting daily allows continual verification of sensor node integrity, while still enabling the visualization of data in a tempo that reflects the weather dynamics. On the other hand, if the data is applied in a close to real-time fashion, a more frequent transmission schedule is needed.

Restricting the frequency of communication holds merits for the sensor node. Firstly, it allows the communications module to power down while not in use. Secondly, it enables batch sending of sensor data. For every payload sent to the server there is a fixed amount of networking overhead, which is why sending larger payloads will reduce the total amount of bytes transmitted.

In section 3.2 it is expressed the desire for a front end user interface for viewing and controlling devices. This in conjunction with the other required networking features hints towards a holistic software solution, i.e. an all-in-one package containing interconnected services, rather than loosely connected software solutions that run as independent instances. A holistic system might be easier to maintain, as updates are applied to the system as a whole. Moreover, it can be easier to ensure that no messages are lost when being exchanged between services. To summarize, a server solution would need the following features:

- Database solution
- MQTT broker
- Upstream and downstream translator (if binary message formats are used)
- Data visualization / Widgets
- Viewing of device attributes
- User authentication



# Implementation

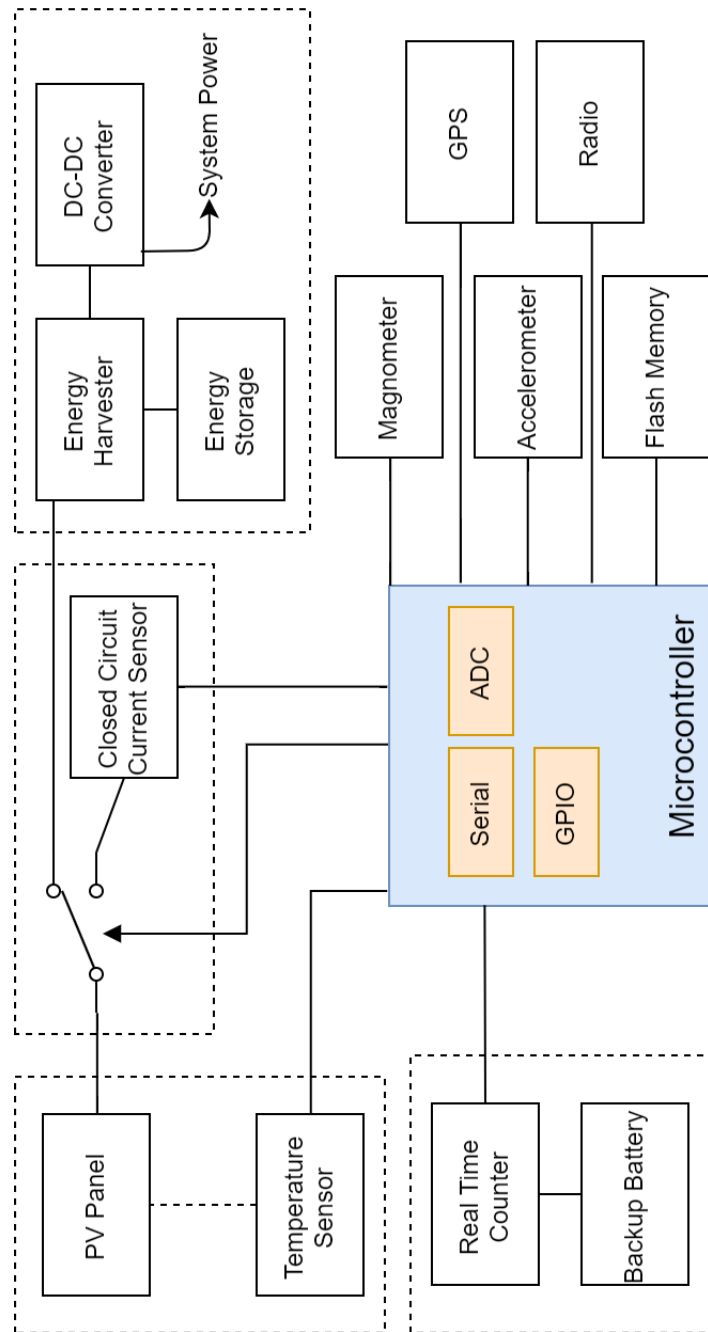
This chapter contains the work done on designing and implementing the sensor node platform. Section 4.1 presents a breakdown of the device functionality and its components, while section 4.2 discusses a general plan for the device firmware.

## 4.1 Sensor Node Hardware

Figure 4.1 shows a proposed system structure based on the points discussed in section 3.1. The suggested implementation relies on using the temperature and short circuit current of the PV panel for estimation of solar production. The solar panel alternates between serving as a component in the closed circuit current sensor and as the input to an energy harvester circuit. The energy harvester is responsible for managing battery charging, and forwards the power output to the DC-DC converter that ensures a steady voltage supply to the system.

Further, there is included an extra battery that serves as a backup for the real time counter, such that the system time is not easily lost. Next, the magnetometer, accelerometer, and GPS are available to the microcontroller, such that the sensor node can determine its orientation and position. Finally, the flash memory is for storing unsent sensor data, and the radio modem is for establishing the wireless link.

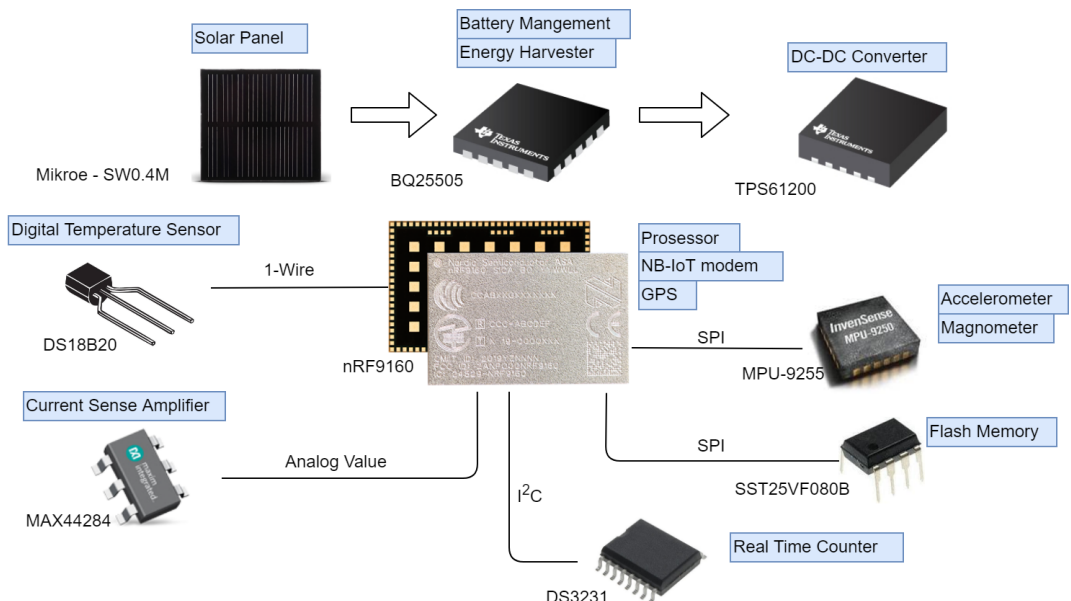
For this project, it is of interest to look at designs using NB-IoT or LoRa for communication. Two different design proposals are made, and are presented in section 4.1.1. The NB-IoT based design has been the focus during testing.



**Figure 4.1:** Proposed system structure.

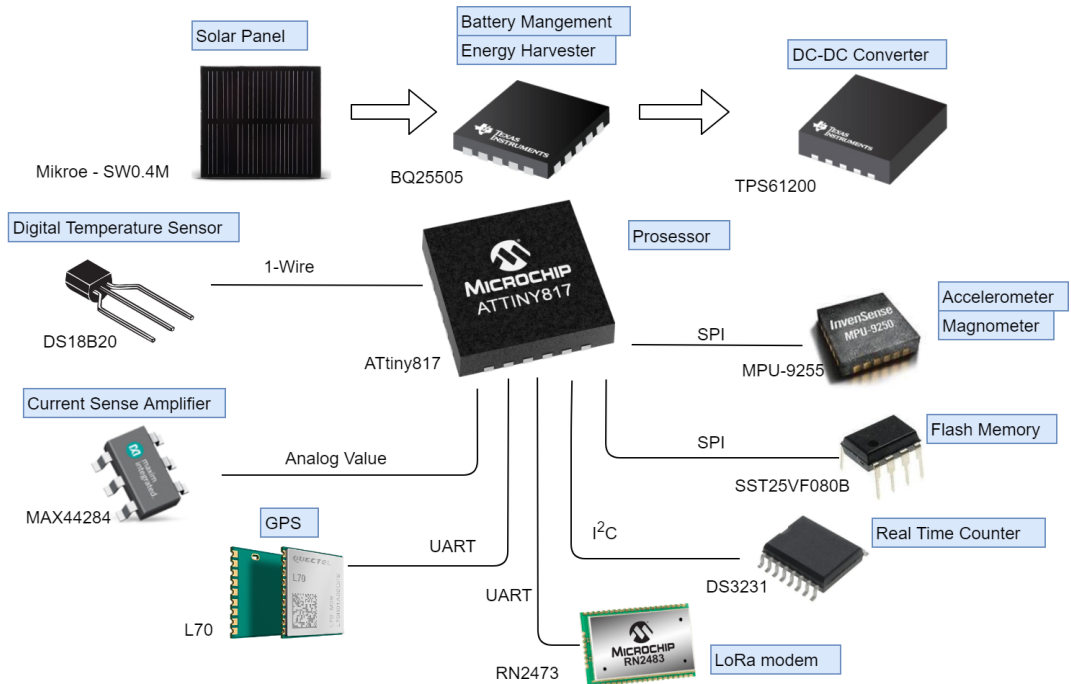
### 4.1.1 Main Components

Figure 4.2 shows the main components for the suggested NB-IoT design. The nRF9160 was chosen as the central unit. It is a low power System-in-Package (SiP) that integrates a NB-IoT and LTE-M capable modem, in addition to having a GPS receiver. It incorporates an Arm Cortex-M33 processor that runs the light weight real-time operating system zephyr. Moreover, the microcontroller has a large amount of peripherals, such as GPIO, event systems, PWM, SPI, timers, TWI, UART, and watchdog timers [13].



**Figure 4.2:** Main components overview for nrf9160 based design. Product images are from mikroe.com, no.mouser.com, ti.com, and nordicsemi.com.

Similarly, figure 4.3 shows the primary components of the LoRa design. The devices used are mostly the same, although, here the central processing unit is the 8-bit microcontroller ATtiny817. This device was selected based on the number of pins and peripherals needed. Also, the unit is relatively new, which is an important factor as the low power aspect of the ATtiny series is being steadily improved. Using an 8-bit microcontroller can be an advantage in terms of simplicity for both hardware layout and firmware development. Unlike the nRF9160, the ATtiny817 does not have radio or GPS capabilities. Thus, these features are introduced using both an external GPS and LoRa modem chip.



**Figure 4.3:** Main components overview for ATtiny817 based design. Product images are from [mikroe.com](http://mikroe.com), [no.mouser.com](http://no.mouser.com), [ti.com](http://ti.com), [quectel.com](http://quectel.com), and [microchip.com](http://microchip.com).

Ideally, all the components would be fitted on to a single circuit board as the final product. This would provide a better premise for designing a housing for the electronics, and provide a way to more easily mass produce units. Figure 4.4 shows how the form of a complete implementation is envisioned. However, in advance of making a full scale implementation, it is desirable to verify the design. This can be done by evaluating modules of the system separately.

Several of the chosen parts are only available in surface mounted packages. This makes prototyping and testing difficult, as there is no good way of connecting to the parts without a PCB. Hence, for some of the modules, development boards with the component already mounted was obtained for testing purposes. Most notably, the development kit for the nRF9160 is used. The development kit includes a debugger IC which is necessary for programming and communicating with the nRF9160 chip. Moreover, the microcontroller has a difficult footprint to hand solder, and the analog design required for a well tuned antenna can be complex.

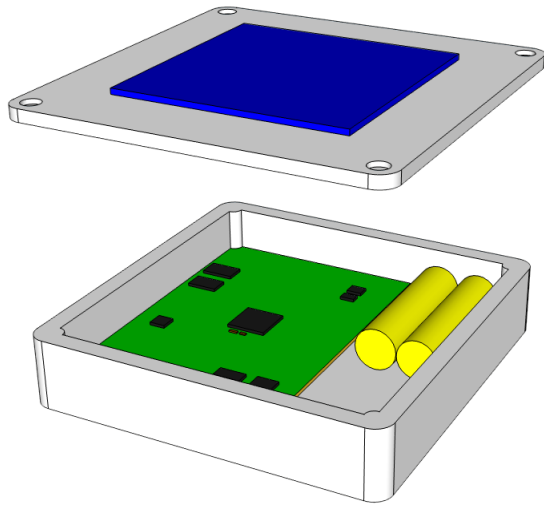


**Figure 4.4:** A visualization of what a finalized implementation might look like.

### Component Details

To begin, the IC DS3231 is selected for the role of external real time counter. The component has an internal crystal with temperature correction, and features an I<sub>2</sub>C interface for reading and writing time. Time can be requested in different formats, e.g. human readable dates or raw timer count. Most importantly, the device has a separate input for a backup power supply input, as can be seen in figure 4.5. In addition, its has a low time-keeping current that is typically  $0.84\mu\text{A}$ . This component should be sufficient to uphold the time drifting requirement 3 from list 3.1, as it has a worst case drift of 0.3 seconds per day [4]. The ZS-042 PCB was acquired for testing purposes, although this board has energy spending elements such as a power indicator LED.

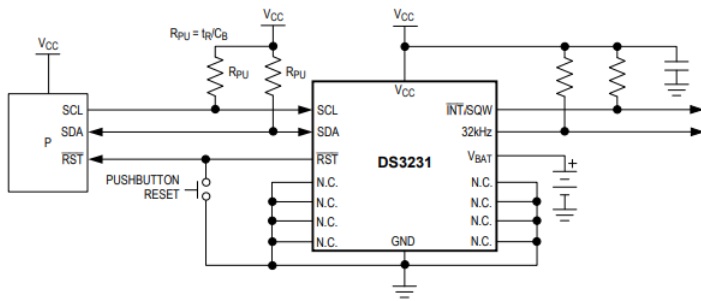


**Figure 4.5:** Typical application of the DS3231 real time counter, as suggested by its datasheet [3].

Next, the IC MPU-9255 provides the measurements used for orientation. The chip was picked for fulfilling both the need for a magnetometer and a accelerometer. Moreover,

the device is featured in several projects that are documented online, that serves as useful reference material for developing firmware. It also has the functionality to enter a power saving mode, and to individually disable unused sensor peripherals [10]. In this project, SPI is chosen for communication, although I<sup>2</sup>C is also supported. The GY9255 module was obtained for the purpose of testing the MPU-9255 component.

Furthermore, the SST25VF080B flash memory was chosen as the external non-volatile memory device. It can hold 1MB of data, and has a typical endurance of 100,000 write cycles. Hence, for instance, given a sample size of 10 bytes and a sample interval of 10 seconds, the chip is able to hold about 11 days worth of samples. The endurance of the memory sectors is considered not an issue, as even if only a single 4KB sector is used, the sector would typically last for 12 years. The device uses an SPI interface, and in addition has a low standby power consumption of 5  $\mu$ A [21]. This component is available in dual in line package type that is compatible with a breadboard, thus, a PCB is not needed for testing.

For temperature measurement, the digital thermometer DS18B20 with the TO-92 package type is attached to the solar panel as seen in figure 4.6. The thermometer has single line for two-way serial communication, and is designed to use 1-Wire protocol. Also, it can measure temperatures in the range of -55°C to 125°C with a maximum 12-bit resolution. In its datasheet, the accuracy is reported to be  $\pm 0.5^\circ\text{C}$  when operating in ranges -10°C and 85°C [3]. The component was selected mostly for being easy to obtain in addition to having detailed documentation. An advantage of dealing with digital thermometers is removing the need to scale the input signal to fit the range of the microcontroller ADC. Furthermore, the device features a standby mode to optimize power saving, which can be controlled through the serial interface.

The BQ25505 energy harvester IC and the TPS61200 DC-DC converter are used in the design of the power module. In addition, the MAX44284 amplifier is the basis for the solar panel current measurement. These modules are explored in section 4.1.2 and 4.1.3.

In the LoRa design, the central processing unit does not contain GPS and radio functionality. These must thus be added as separate components. For LoRa communication, the RN2483 LoRa modem is chosen, as it has low power consumption and is compatible with the system voltage. The chip communicates using a UART command interface. By issuing a command the unit can be put into a low power state. An advantage of the RN2483 is that it contains a LoRaWAN protocol stack, and handles the lower level communication [17]. The LORA CLICK development board was acquired for testing.

For GPS, the Quectel L70 is selected. This device is designed for low power applications, and features low current drain for both active and hibernation modes. Further, the chip has a UART interface and communicates using NMEA 0183, which is a simple ASCII protocol commonly applied in GPS and similar devices.

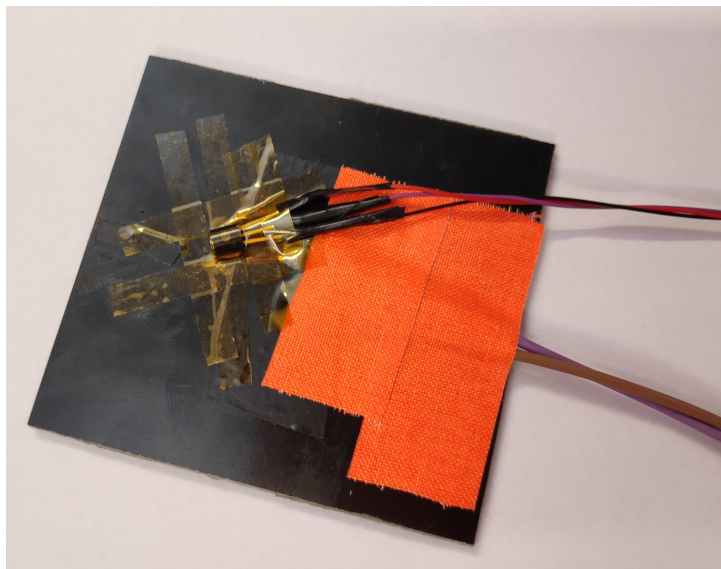


**Figure 4.6:** Digital thermometer DS18B20 attached to the backside of the solar panel using thermal paste and kapton tape.

### Wiring Schematic

In figure 4.7 the wiring schematic for the NB-IoT design can be seen. The nRF9160 chip has more pins than what is needed for this project, however, the development board claims some of them for demonstrative features that are present on the board. Thus, the wiring has been adapted to the development kit, which explains the somewhat non-consecutive configuration. A merit of the nRF9160 is the ability to reroute signals internally, i.e. special feature peripherals such as SPI can be matched to a pin configuration through firmware.

Further, in figure 4.8 the wiring schematic for the LoRa design is shown. This configuration uses most of the pins that are available for the ATtiny817 device. In general, the microcontroller has rigid rules for routing, as some peripherals are only available through a given set of pins. For this design, the UART peripheral of the microcontroller is shared between the LoRa modem and the GPS device, using an internal muxing feature of the ATtiny817. This means that the central unit can only communicate through UART with either component at a time. This should not pose a problem, as the positioning feature is mainly intended for use during initial setup.

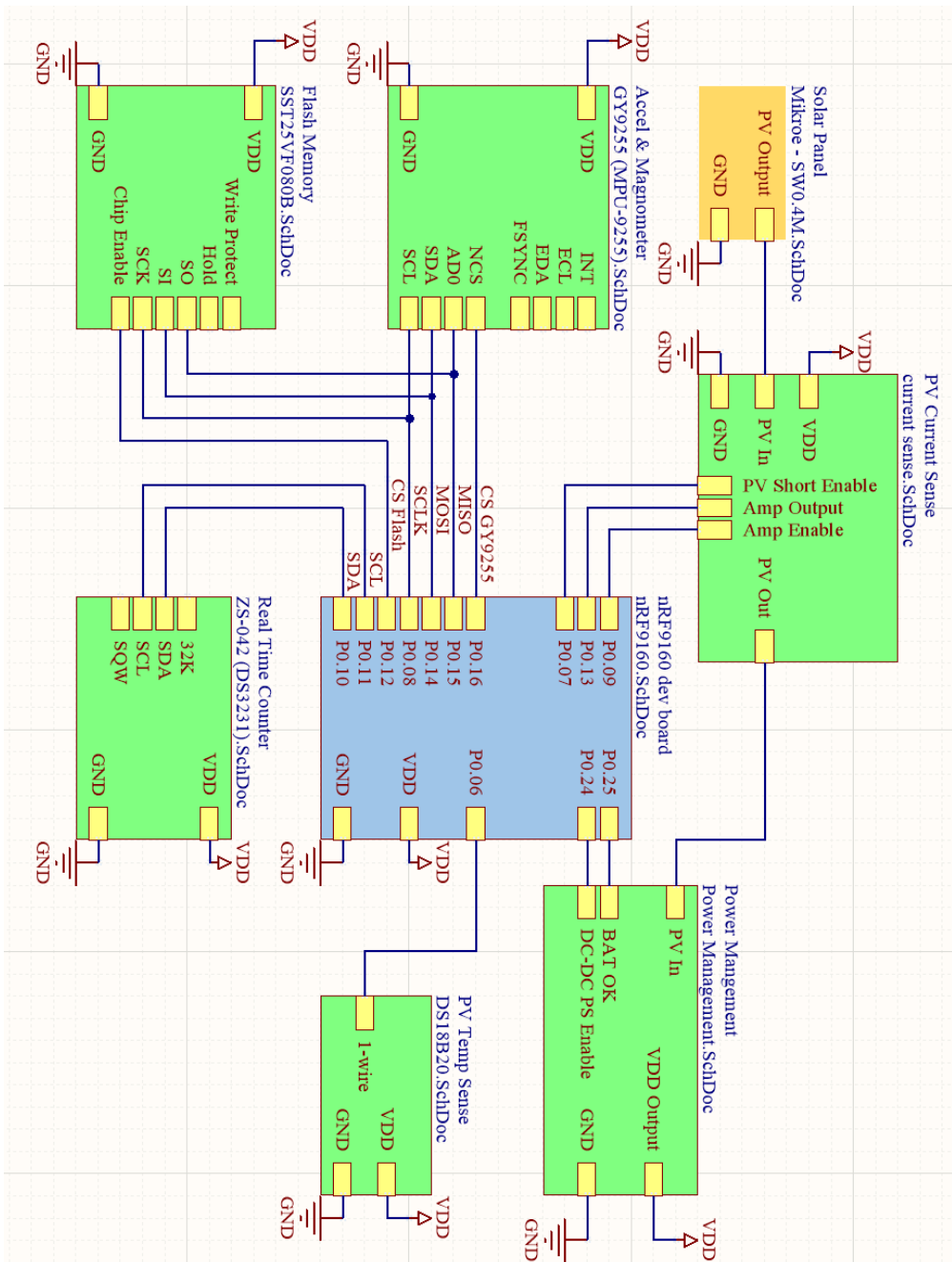


Figure 4.7: Wiring schematic for the NB-IoT design.

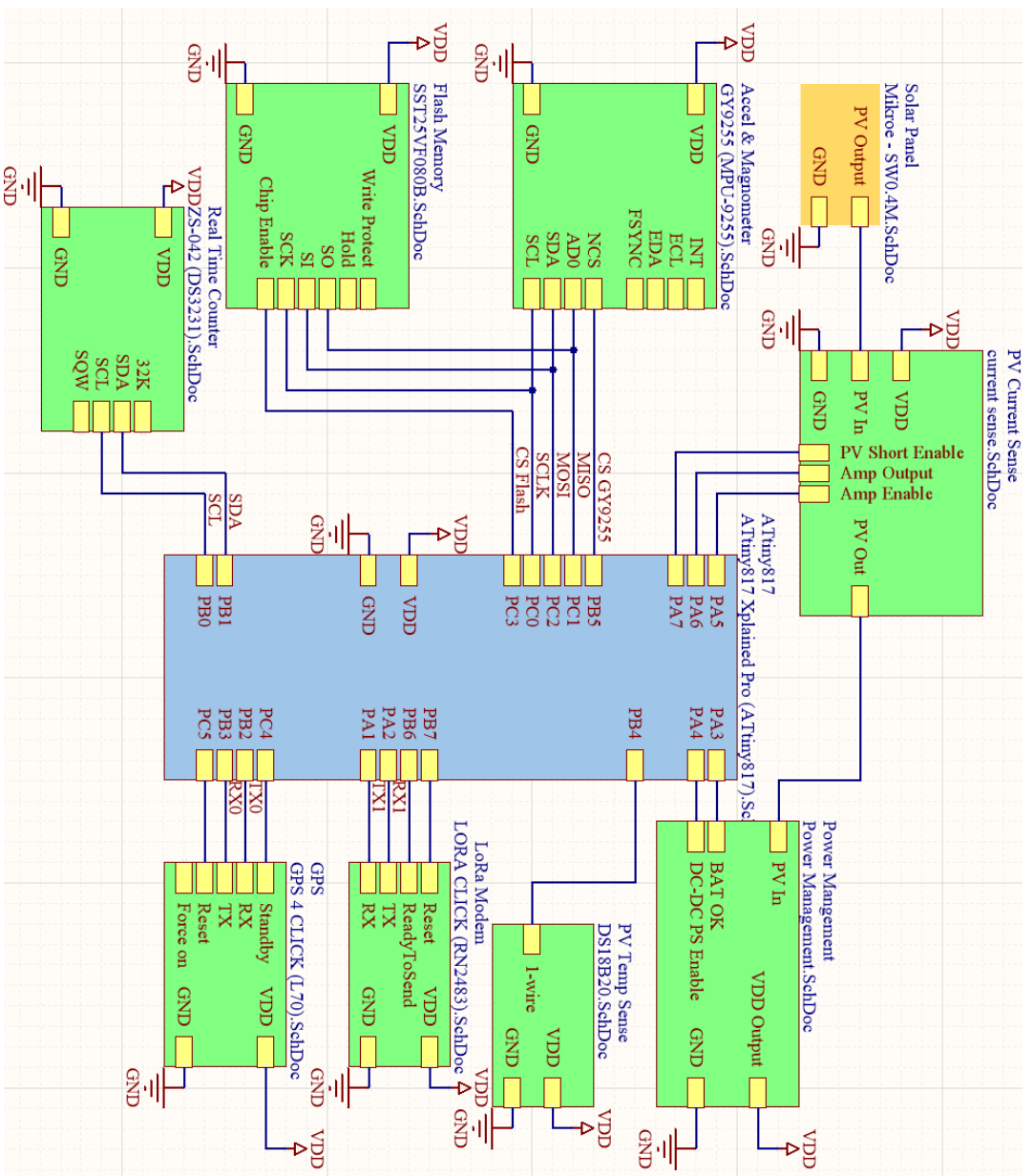


Figure 4.8: Wiring schematic for the LoRa design.

### 4.1.2 Closed Circuit Current Measurement

In order to give an estimate of PV panel production, the short circuit current of the panel can be used together with the panel operating temperature. This means there is a need to

implement a current sensing circuit, and a thermometer should be included. Also, since PV panels are costly and take up space, the circuit can share the panel used with the energy harvester.

To achieve this, a shunt resistor is placed in series at the output of the PV panel, such that any current passing out of the panel will pass through the resistor first. The voltage drop over the resistor is then amplified using the low-power current-sense amplifier MAX44284F. Figure 4.9 shows the typical application circuit for the component, which also describes the basis of this implementation.

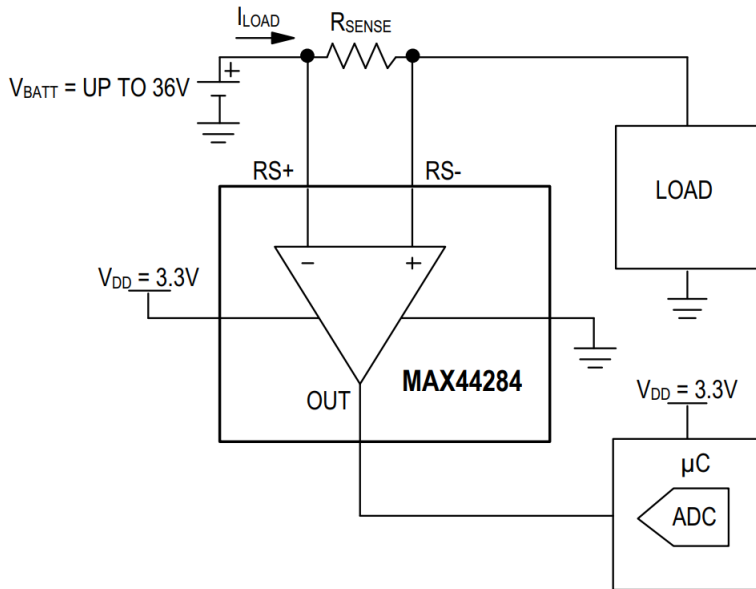


**Figure 4.9:** Typical application circuit for MAX44284 [9].

The MAX44284F amplifier was chosen due to being easy to implement and interface with. It is also compatible with the system power supply voltage,  $V_{dd} = 3.3V$ , and has the option to enter an idle, low power, mode.

According to the component description of the amplifier [9], the input voltage sense range is given by the following formula:

$$V_{sense\_range} = \frac{V_{dd}}{G} \quad (4.1)$$

Where  $V_{dd}$  is the voltage supply, and  $G$  is the gain used in the amplification. For our system,  $V_{dd}$  is assumed 3.3V, while the gain of the amplifier is preconfigured based on the

MAX44284 variant. As seen in table 4.1, there are four available fixed gain options to choose from.

**Table 4.1:** MAX44284 variants. Assumed  $V_{dd} = 3.3V$

Name	Gain	$V_{sense\_range}$
MAX44284F	50	66mV
MAX44284H	100	33mV
MAX44284W	200	16.5mV
MAX44284E	500	6.6mV

Next, the solar panel chosen for this system has a maximum short circuit current of 105mA [22]. The shunt resistor value must be chosen such that the voltage drop over the resistor does not exceed the voltage sense range of the amplifier, while also ensuring that as much as possible of the range is used. By using Ohm's law, the largest possible resistor value can be found as shown in eq. 4.2.

$$\begin{aligned}
 V_{shunt\_max} &= V_{sense\_range} = I_{short\_circuit} * R_{shunt} \\
 \Rightarrow R_{shunt} &= \frac{V_{sense\_range}}{I_{short\_circuit}}, \text{ substitute using eq. 4.1} \\
 \Rightarrow R_{shunt} &= \frac{V_{dd}}{I_{short\_circuit} * G}
 \end{aligned} \tag{4.2}$$

Hence, in the case of MAX44284F with gain 50, we have  $R_{shunt} \approx 0.629\Omega$ . The value is then rounded down to the nearest available resistor value,  $R_{shunt} = 0.62\Omega$ . This gives a maximum voltage drop of 65.1mV over the shunt resistor.

A prototype circuit board was designed with the purpose of testing the design as a separate module, its schematic is shown in figure 4.10. The connector J1 is the PV panel input, which is passed through the shunt resistor, R1. The circuit features a N-channel MOSFET, Q1, that can be opened to short the PV panel to ground. Otherwise, when the transistor is closed, the current will flow towards connector J4 which is connect to the energy harvester. For this implementation, the transistor PSMN1R2-30YLD is used, mainly because of its low drain-source resistance of about  $1m\Omega$  and a small leakage current  $< 1\mu A$  [42]. As a side note, a pair of extra connectors were added to the circuit board to allow manual wiring of the traces.

Furthermore, the module requires three connections to the microcontroller. There are two control signals, where one is for operating the MOSFET. The other one is directed to the enable pin of the amplifier, which allows the microcontroller to put the component in a power saving mode. Finally, the module provides an analog signal which is the amplified voltage drop over the shunt resistor. The signal will be within the range of 0 to  $V_{dd}$ , and is read with an ADC on the microcontroller. When converting from output voltage to current, equation 4.3 can be used. The accuracy of the output voltage is described by eq. 4.4 [9]. At  $25^\circ C$ , the gain error is typically about 0.05% and the  $V_{offset\_voltage}$  is about  $2\mu V$ . Thus, the maximum error at 105mA for  $V_{out}$  is  $\pm 1.6mV$ , which translates to  $53\mu A$  using equation

4.3.

$$V_{out} = G * (R_{shunt} * I_{shunt})$$

$$\Rightarrow I_{shunt} = \frac{V_{out}}{G * R_{shunt}} \quad (4.3)$$

$$V_{out} = (G \pm G_{error}) * V_{sense} \pm (G * V_{offset\_voltage}) \quad (4.4)$$

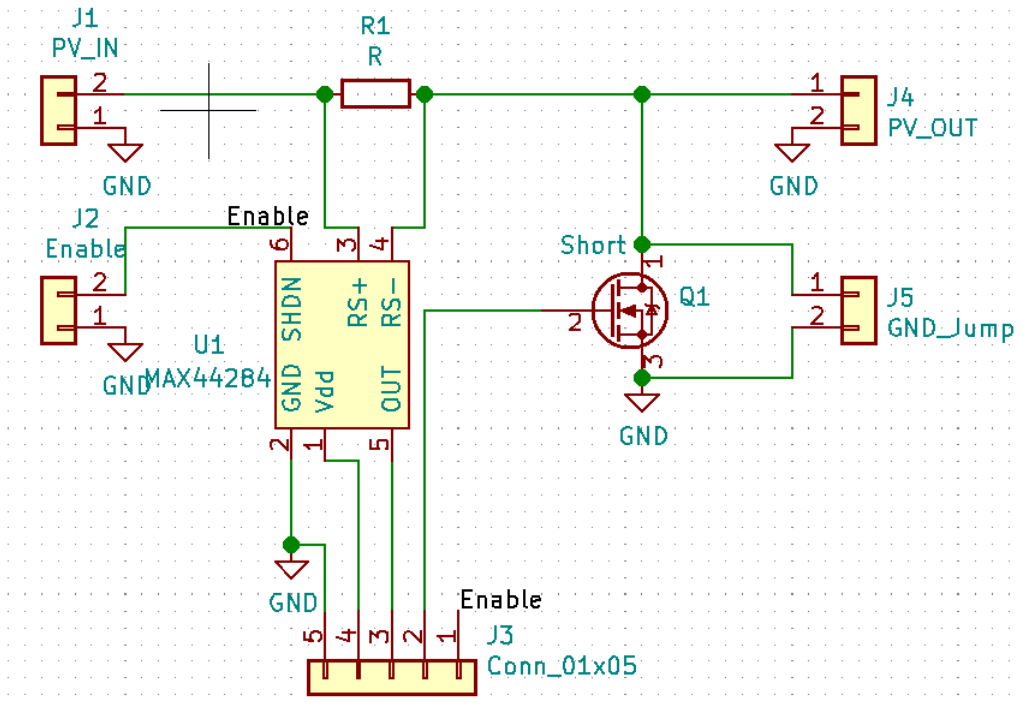


**Figure 4.10:** Schematic for the current sense circuit.  $R1 = 0.62\Omega$ .

### 4.1.3 Power Module

The power module consists of an energy harvester module, and a DC-DC booster. The combined schematic of both parts can be found in figure 4.14.

#### Energy Harvester & Storage

The implementation of the energy harvester module is based on the energy harvesting IC BQ25505, which is directed towards applications that rely on thermal or solar electric

generators. Its main features is extracting energy with the help of a configurable MPPT sampling network, battery charging management, and storage element multiplexing. Figure 4.11 shows a simplified view of the implementation. The PV panel is the input to the energy harvester, that is used to charge the secondary battery. Further, there is an additional non-rechargeable battery that serves as backup energy storage. The primary battery is automatically selected when the secondary battery voltage drops below a set level.

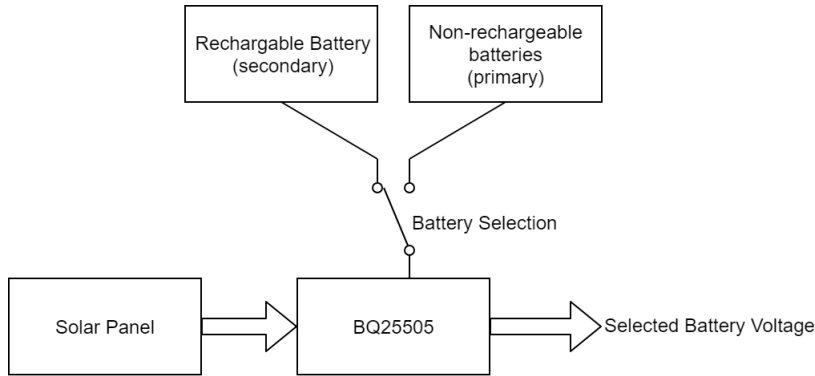


**Figure 4.11:** Simplified illustration of BQ25505 application.

Figure 4.12 shows the schematic for the solar harvester circuit, which was made based on the example circuit for solar harvesting in the BQ25505 datasheet [33]. It was designed with the intention of making a single circuit board to test and verify the power module. To begin, there are three connectors present, for connecting the PV panel, primary, and secondary battery. Furthermore, there is a resistor network labeled ‘Battery Voltage Protection Configuration’, which programs the battery charging management of the BQ25505. In order to find reasonable resistor values, the rechargeable battery properties must be known. The following parameters must be determined:

- Battery overvoltage
- Battery lower threshold (battery OK)
- Battery hysteresis voltage

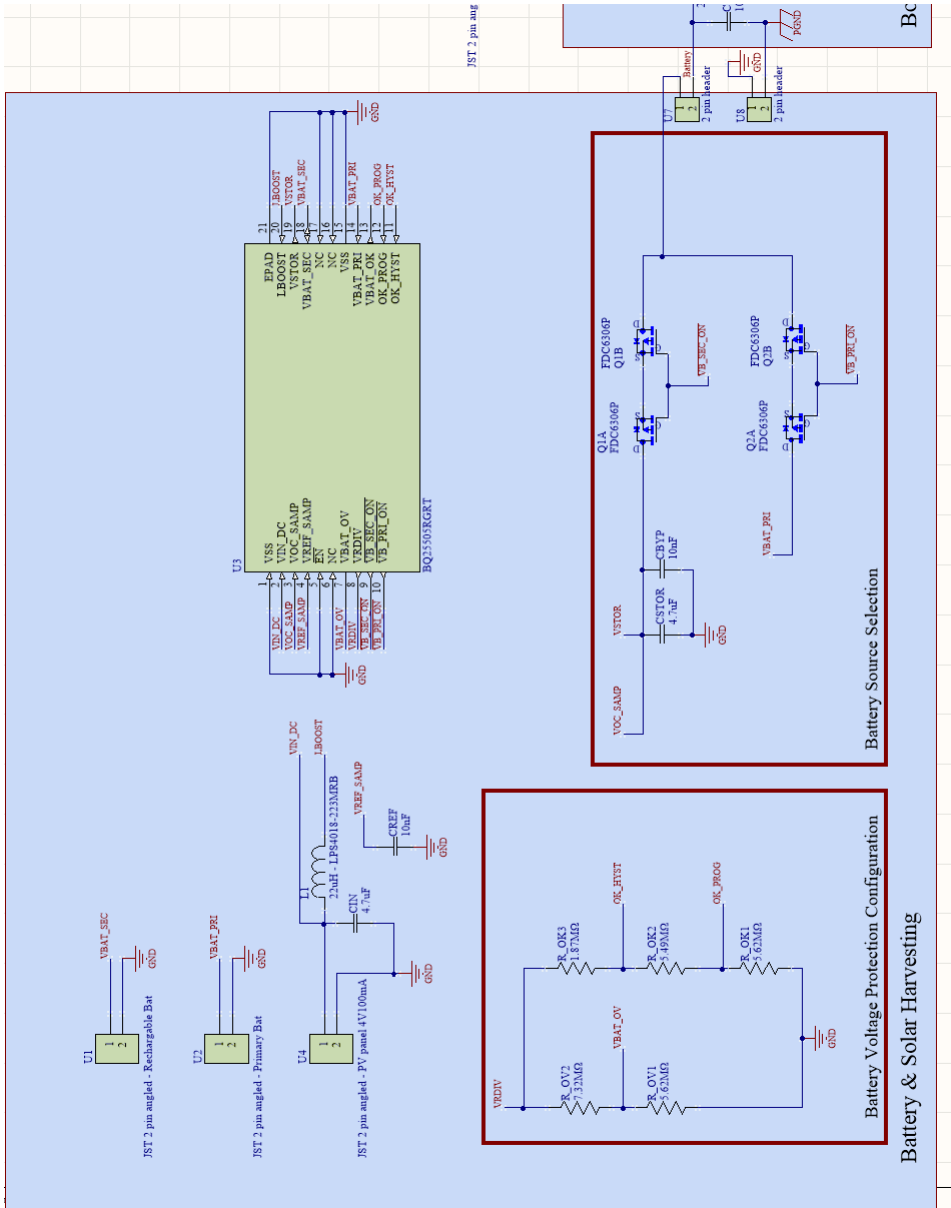


Figure 4.12: Schematic for a solar harvesting circuit based on BQ25505.

For this implementation a 103450AR2-1S-3M lithium-ion battery is used with the test circuit board. The values  $V_{bat\_overvoltage} = 4.2V$ ,  $V_{bat\_ok} = 2.39V$ , and  $V_{bat\_hyst} = 2.8V$  [31] are used as a basis for programming the battery charging. Resistor values are then found by applying the formulas found in the BQ25505 datasheet as shown below.

$$R_{sum\_OV} = R_{OV1} + R_{OV2} = 13M\Omega$$

$$R_{OV1} = \frac{3}{2} * \frac{R_{sum\_OV} * V_{bias}}{V_{bat\_overvoltage}}, \text{ where } V_{bias} = 1.21V$$

$$\Rightarrow R_{OV1} \approx 5.618M\Omega$$

$$\Rightarrow R_{OV2} \approx 7.382M\Omega$$

$$R_{sum\_ok} = R_{OK1} + R_{OK2} + R_{OK3} = 13M\Omega$$

$$R_{OK1} = \frac{V_{bias} * R_{sum\_ok}}{V_{bat\_hyst}}, \text{ where } V_{bias} = 1.21V$$

$$R_{OK2} = \left( \frac{V_{bat\_ok}}{V_{bias}} - 1 \right) * R_{OK1}$$

$$\Rightarrow R_{OK1} \approx 5.618M\Omega$$

$$\Rightarrow R_{OK2} \approx 5.479M\Omega$$

$$\Rightarrow R_{OK3} \approx 1.904M\Omega$$

Further, the values are rounded to the nearest available resistor value, yielding the result shown in table 4.2.

**Table 4.2:** Resistor values for battery charge mangement programming

Resistor	Value
$R_{OV1}$	$5.62M\Omega$
$R_{OV2}$	$7.32M\Omega$
$R_{OK1}$	$5.62M\Omega$
$R_{OK2}$	$5.49M\Omega$
$R_{OK3}$	$1.87M\Omega$

Next, there is the configuration of the MTTP function of the BQ25505. The IC periodically samples the open current voltage of the solar panel. It does this by periodically disconnecting the panel from its internal boost charger, which is normally used to charge the battery. The sampled voltage is then used as a reference for the optimal operating point. In this implementation the VOC\_SAMP pin is connected to the VSTOR pin such that the maximum power point is set to 80% of the open circuit voltage, which is a typical value for solar panels [33].

Finally, for the primary battery, two AA alkaline batteries in series are used. Alkaline batteries have a relatively low discharge rate, and are commonly available. Although they might not hold much charge compared to other solutions, the primary battery is mainly intended to keep the system running a short period of time after the rechargeable battery drops below the  $V_{bat\_ok}$  threshold.

### DC-DC Converter

The DC-DC converter is responsible for converting the battery voltage level to the system voltage,  $V_{dd} = 3.3V$ . For this implementation the synchronous boost converter TPS6120 is applied. One of the main advantages of the IC is the ability to autonomously switch between boost mode and down conversion mode. The system target  $V_{dd}$  lies inside of the battery voltage range, i.e. the battery can have both higher and lower voltages than the system. The IC can handle inputs in range 0.3V to 5.5V [32].

Figure 4.13 shows the suggested schematic for the implementation, which is based on the circuit example in the TPS61200 datasheet [32]. An important feature of the converter is the power saving mode that can be enabled to increase conversion efficiency for lighter loads. Note, that some connection headers are added for ease of access during testing.

The voltage divider, R1 and R2, is used to program the output voltage of the converter. The IC will continue to increase the output until the input voltage of the FB pin is 500mV. Moreover, it is recommended to keep the R2 value lower than 200k $\Omega$ . Hence, for a selected R2 of 180k $\Omega$ ,  $V_{out} = 0.5V$ , and  $V_{dd} = 3.3V$ , formula 4.5 can be used to show that a  $R1 = 1.008M\Omega$  is needed. R1 is then rounded to 1M $\Omega$ .

$$\begin{aligned} \text{Voltage divider output: } V_{out} &= \frac{V_{dd} * R2}{R1 + R2} \\ \Rightarrow R1 &= \frac{R2 * (V_{dd} - V_{out})}{V_{out}} \end{aligned} \quad (4.5)$$

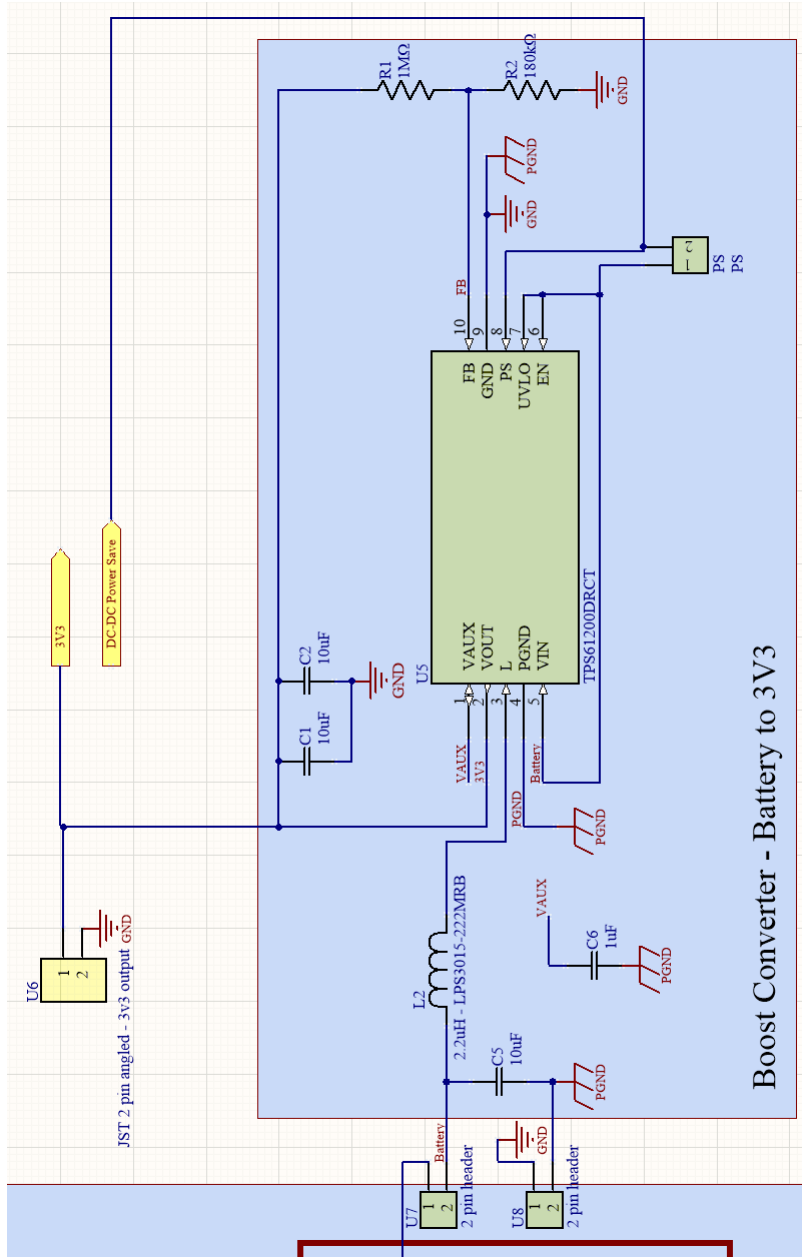
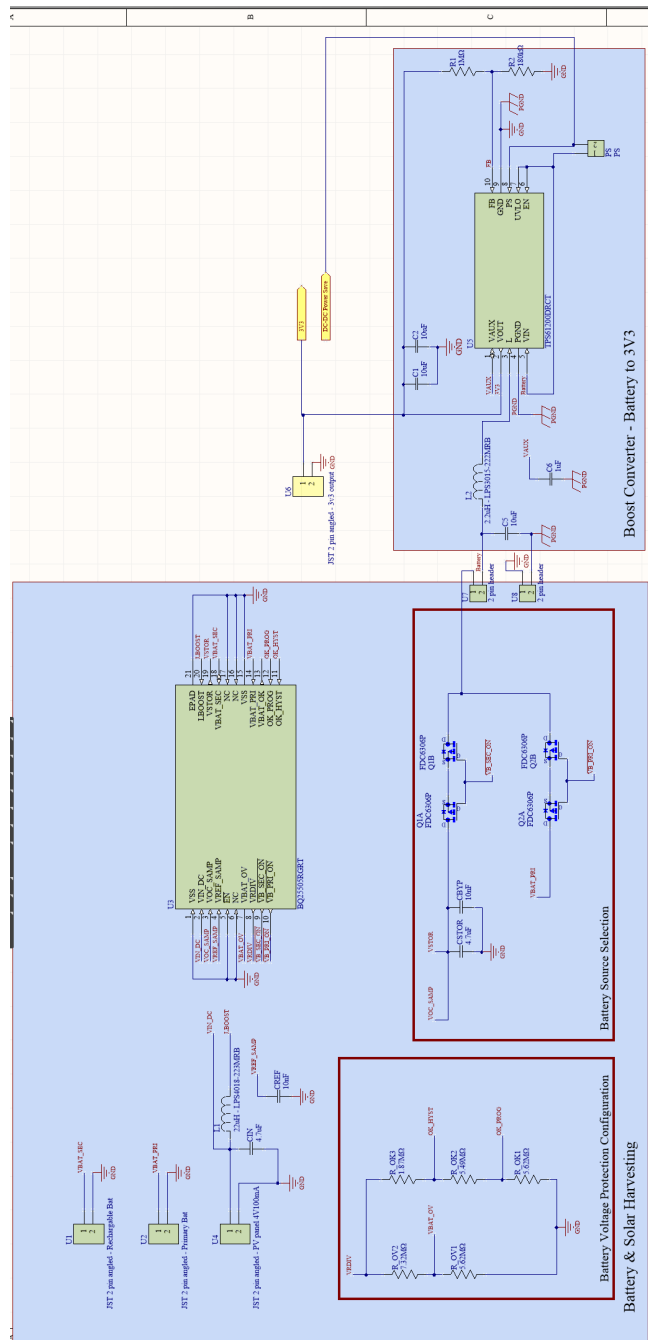


Figure 4.13: Schematic for DC-DC converter based on TPS61200.



**Figure 4.14:** Power module circuit schematic.

#### 4.1.4 PCB Design

A PCB was designed and produced for the power module and current sense circuit, based on the schematics presented in figures 4.14 and 4.10. Primarily, the computer-aided design tool Altium Designer was used for making most schematics and layouts. KiCad was used for the current sensor PCB. Figure 4.15 shows the routing used for the power module circuit. Figure 4.16 displays a printed board of an earlier revision of the design, which was used for testing. The layout for the current sensor is presented in figure 4.17, and a picture of the board is shown in figure 4.18.

Extra care was taken when designing the layout for the power module by sticking closely to the guidelines given in the component datasheets. Switching power supplies are sensitive to the circuit routing, as they can experience issues with regulator stability and electromagnetic interference if layout is not done carefully [32]. For reference, the layout examples for the BQ25505 and TPS61200 are included in figures 4.20 and 4.19.

Due to the circuit board having small traces, the power module PCB was fabricated using a professional PCB production service. The current sensor has a simpler design, its PCB was produced locally using acid etching equipment.

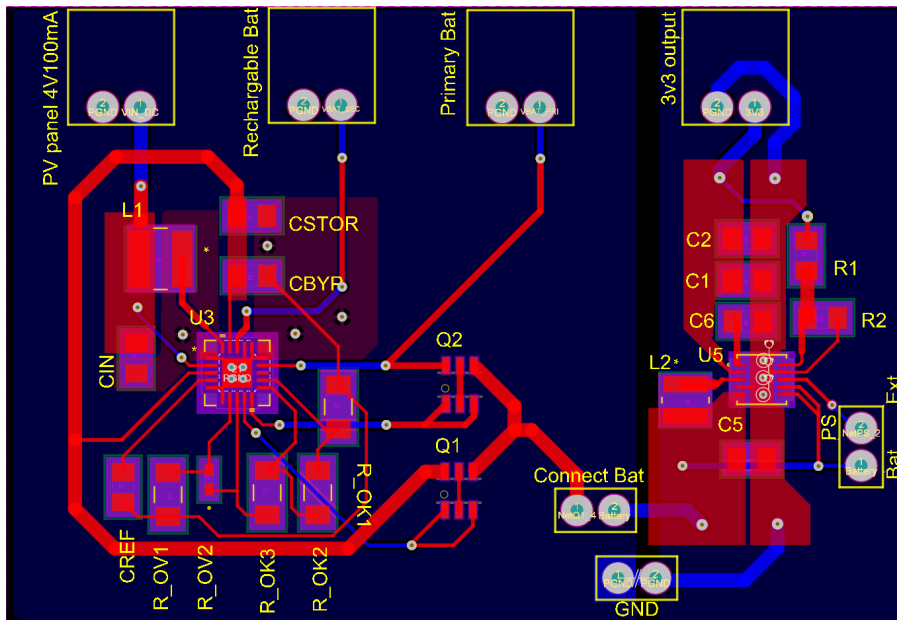
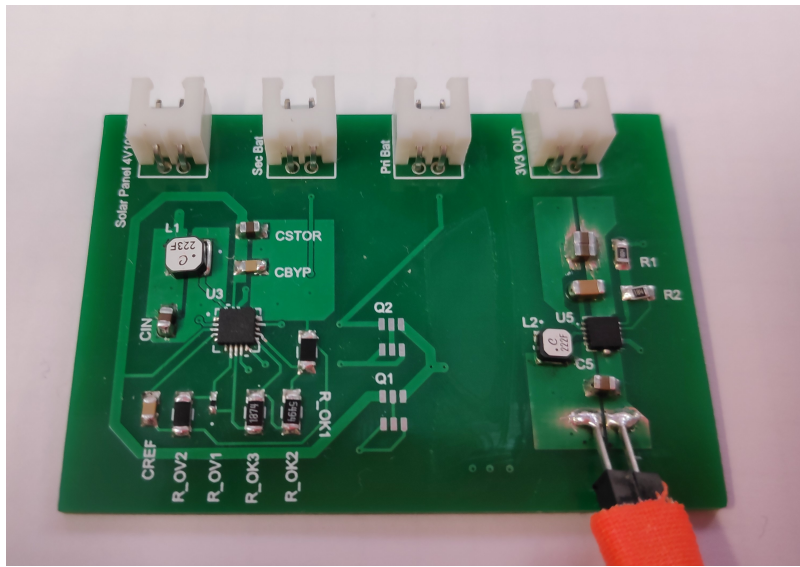
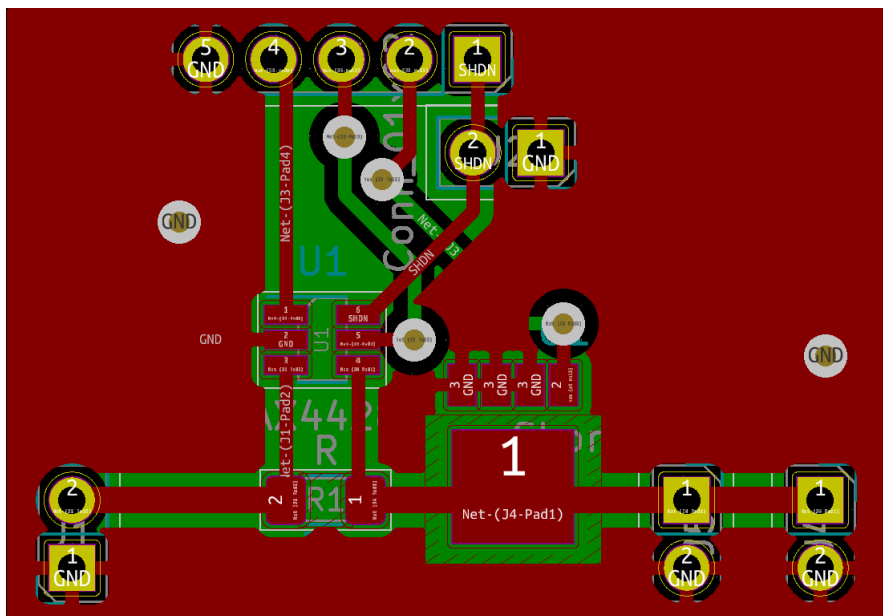


Figure 4.15: Power module circuit layout.



**Figure 4.16:** Power module PCB that was used for testing.



**Figure 4.17:** Power module circuit schematic.



**Figure 4.18:** PV current sensor PCB.

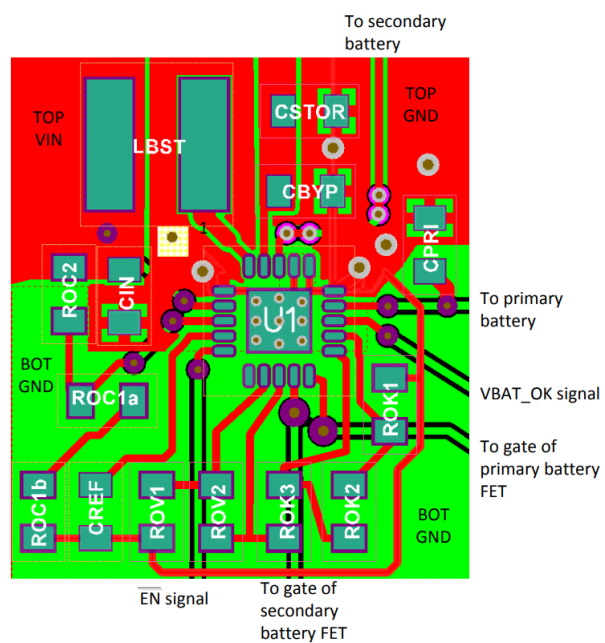


**Figure 4.19:** Layout reference for BQ25505 [33]

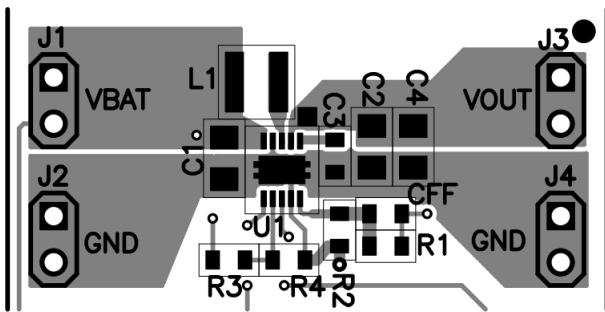


Figure 4.20: Layout reference for BQ25505 [32]

## 4.2 Software

In this section a general structure for the software design is proposed. The suggestions presented here are not fully implemented. In addition, the details of the proposed design in section 4.2.1 is made with NB-IoT in mind. While the basic concept can be applied for LoRa as well, the throughput and maximum allowed payload differs from NB-IoT. Moreover, for LoRa the IP protocol is handled at the gateway, rather than directly from the device, such that the amount of transmitted bytes will be different.

### 4.2.1 Sensor Node Firmware

The basic functionality of the sensor node is being able to periodically send the observed sensor data for the solar panel to a central server. In general, for battery or energy harvesting based IoT nodes, optimizing the use of available power is one of the key challenges. In terms of software, it is possible to reduce the power consumption of the system by powering down whichever feature is not currently in use. Figure 4.21 shows a simplified model of the suggested program flow, where the sensor node has a read-communicate-sleep cycle.

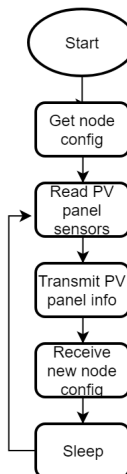


**Figure 4.21:** Simplified model of the proposed sensor node mainloop.

According to specification 4 in the requirement list 3.1, the time between samples and the time between submitting the samples to the server must be configurable. In addition, the sensor node must be able to supply position information if prompted. It is also given that the device should communicate through the MQTT protocol.

Figure 4.22 shows a more detailed model for the proposed program flow. In the diagram, when the device initializes, it begins by contacting the server. Upon making a connection with the MQTT broker, it request the creation of a new persistent MQTT session, and

subscribes to a topic unique for this sensor node. Beforehand, the server should have published a retained message with the node configuration to the topic. Hence, the node will receive the message upon subscribing.

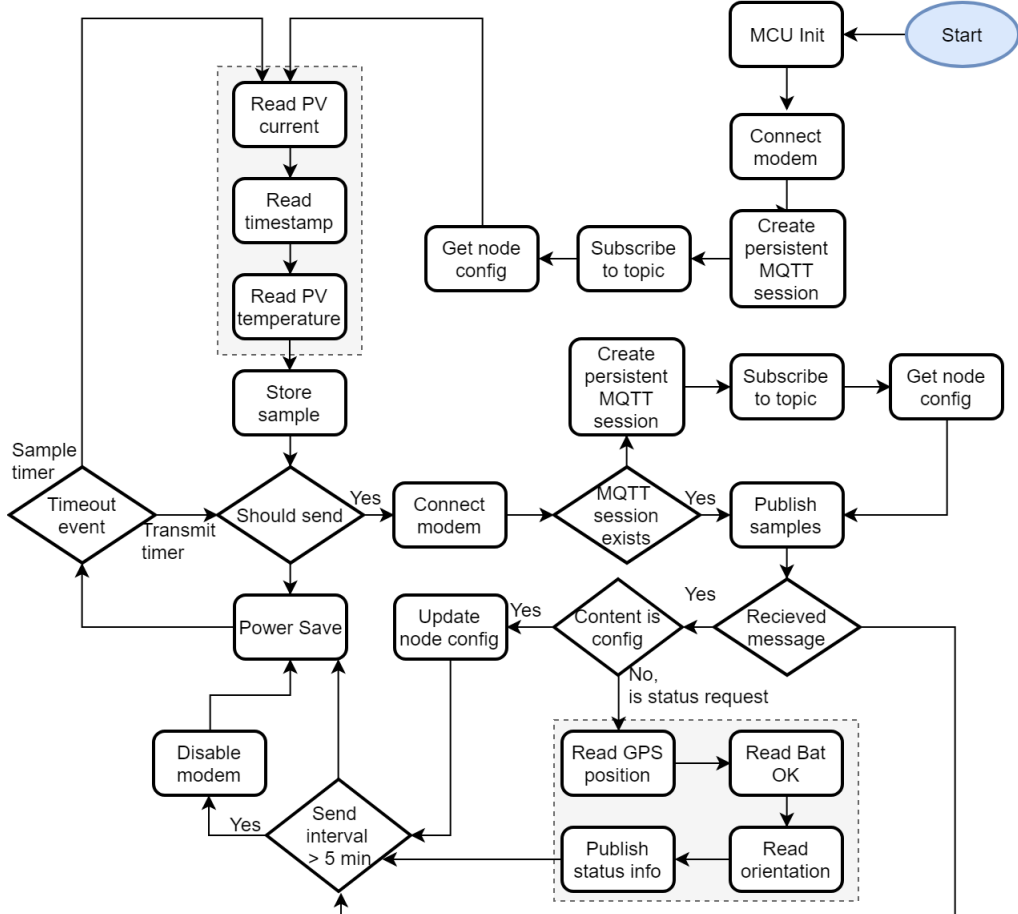


**Figure 4.22:** Model of the proposed sensor node mainloop.

Further, the node enters the read-transmit-sleep cycle, where a timer is used to wake the system from power save mode. Based on which interval timing triggered an event, the sensor node will either start the sampling process, or proceed directly to communicating with the server. When connecting to the MQTT broker, the node can ask for the previously created MQTT persistent session, which saves the device from retransmitting all of the session parameters. The node can then proceed to publish its retained sample data.

Moreover, using a persistent session will ensure that messages posted while the device is offline will be delivered when the session is resumed. Messages received from the server

will either contain configuration data, or it will be a request for the node to publish its orientation data. Finally, the model includes a decision at the end of the communication for whether the modem should be powered off or if the wireless link should be kept online, based on the frequency of communication. One of the arguments for this behaviour is that the wireless modem can sometimes spend several minutes trying to establish a link. Secondly, the energy spent on establishing a link could be greater than what it would required to maintain it. However, the cost of these actions are not thoroughly explored in this project, i.e. the compare value of 5 minutes in figure 4.22 should be revised.

### Message Structure

For this project JSON encoding is used when exchanging messages between the sensor node and server. This is not an optimal data representation in terms of byte usage, but on the other hand is well suited for prototyping. The main perks of JSON encoding is human readability and that data can be added in any order. In addition, it is widely supported by applications. In a potential later implementation, a binary format might be preferred in order to reduce the total amount of bytes needed.

When committing samples to the server, three values are supplied: the PV panel short circuit current, the temperature reading for the PV panel, and the time of sampling in unix time. The values read from the thermometer and current sense circuit should be converted to Celsius and milliampere before being transmitted, as the server would not necessarily know the bit configuration of the ADCs that were used. A floating point representation should be applied, such that significant digits are not lost through integer conversion.

When converting a floating point number to string, the number of characters can be limited by deciding a fixed amount of decimals. It is known that the current will not typically exceed 105mA, and the temperature is typically within the range of -40°C to 100°C. Hence the first three digits of the float will not go beyond 3 characters. As for the unix time, it is an unsigned 32-bit integer and will not exceed  $(2^{32} - 1)$  in value, i.e. its string representation will always be 10 characters or less. The proposed message format for a sample can be seen below.

```
// Sensor data format
{
  "isc": <Float>,      // short circuit current
  "tmp": <Float>,      // temperature reading
  "ts":  <Integer>     // unix time
}
```

The two first lines is 7 bytes + the length of the floating point string variables, the third line is at most 15 characters, and then there are the two curly brackets enclosing the message. If both floating point numbers are assumed a maximum of 6 characters, a single message has the potential to be 43 characters long. In comparison, a binary form without labeled fields would require 4 bytes for each floating point number and 4 more for the 32-bit

integer, thus, a total of 12 bytes. However, the server would need to know the endianness of the packaged data, in addition to knowing the exact sequence of variables to expect.

Below is the proposed message structure for the sensor node status message and the server response message.

```
// Sensor node status message
{
    "lat": <Float>,      // Latitude      (Decimal Degree)
    "long": <Float>,     // Longitude
    "rotx": <Integer>,   // Relative rotation in x-axis
    "roty": <Integer>,   // Relative rotation in y-axis
    "rotz": <Integer>,   // Relative rotation in z-axis
    "ori": <Integer>,    // Angle of orientation
    "BOK": <Boolean>     // Battery ok
}

// Configuration message from server.
// All fields are not always present
{
    "samp": <Integer>,   // Sample interval
    "send": <Integer>,   // Send interval
    "ts": <Integer>,     // unix time
    "req": <Boolean>,    // request device status
}
```

Although the size of the messages are not optimal, they account only for a part of the bytes needed for communication. For the NB-IoT node to be able to connect to an MQTT broker, it uses the IP, TCP, and MQTT protocol. For every TCP message sent there is 40 bytes of overhead, and every TCP session requires a 3-way handshake at the start and end of the transactions. In addition, there is an overhead for every MQTT message that is sent. In order decrease overhead relative to payload, sending multiple messages in a single TCP payload is advantageous. It follows that for frequent transfers, keeping the connection alive could save both power and bytes.

A simple test was performed where JSON encoded messages were generated and sent from the nRF9160 development board. This was done using the official MQTT library from Nordic Semiconductor [28], and the JSON formatting library available in the Zephyr environment [30]. A server running the CentOS operating system hosting the ThingsBoard open-source IoT platform was used as the MQTT broker [26]. Figure 4.23 shows a snapshot of the user interface, where the GPS position is displayed as a widget.

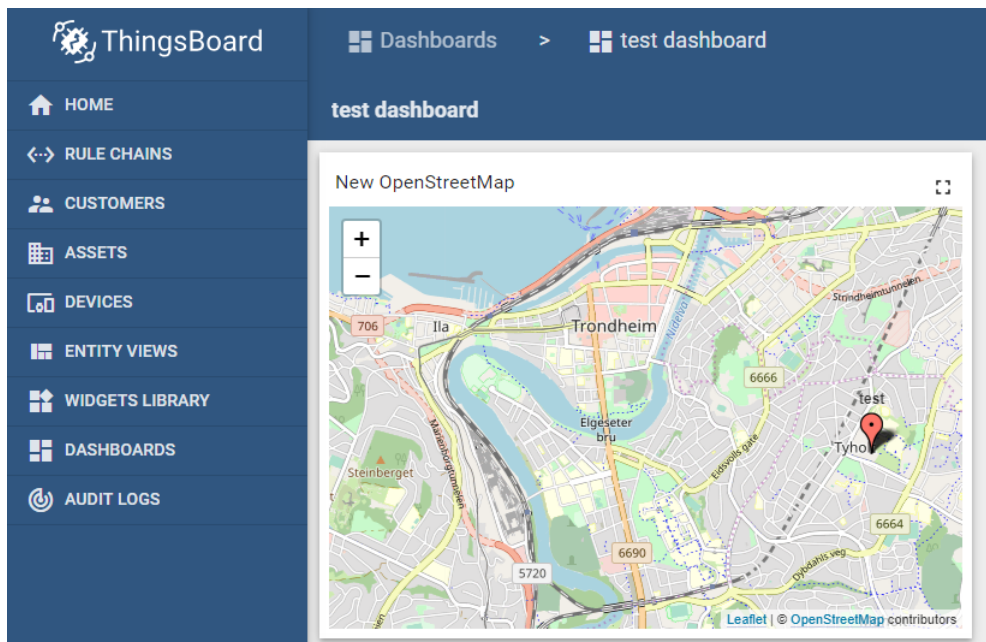


**Figure 4.23:** A screenshot of the ThingsBoard dashboard, showing the received GPS position of the device.



# Chapter 5

## Results & Discussion

During this project we proposed a set of requirements for providing a basis for the embedded design. These were then used to suggest a set of components that could sufficiently cover the design requirements. While the finished product is envisioned as a single PCB, we have here implemented and tested parts of the design as separate modules. In addition, a general description of the device firmware was presented.

The properties of the solar panel was examined by measuring the panels power-voltage curve. A digital adjustable load was attached to the panel, and a 2kW lamp was pointed towards the panel at 2.7 meters distance. By varying the load while measuring both the current and voltage output of the panel, the power-voltage curve was found. This test was done several times, where the panel was tilted at varying degrees towards the lamp to adjust the amount of energy received. The plot in figure 5.1 shows the resulting values, labeled after the short circuit current observed at each tilt position.

For this test, a IT8512A electronic load in constant resistance configuration was used along with a L02000TF 2kW stage lamp. The voltage and current were obtained from the electronic load.

The curve in figure 5.1 has the expected shape of a solar panel. Notably, the optimal working point does not change significantly for different panel angles. This shows that the angle of illumination is significant for power received, but does not change the shape of the curve, instead it works as a scaling factor.

While the lamp used was not characterized an informal comparison was performed, where the panel short circuit current was measured outside on a cloudy day around midday. The highest observed short circuit current for the lamp was around 12mA, while for the outdoor test 14mA was observed. This can indicate that the lamp used was less than optimal for simulating field conditions. During the outside test, the maximum value was found when pointing the panel straight up, which shows that the clouds are a good diffuser that

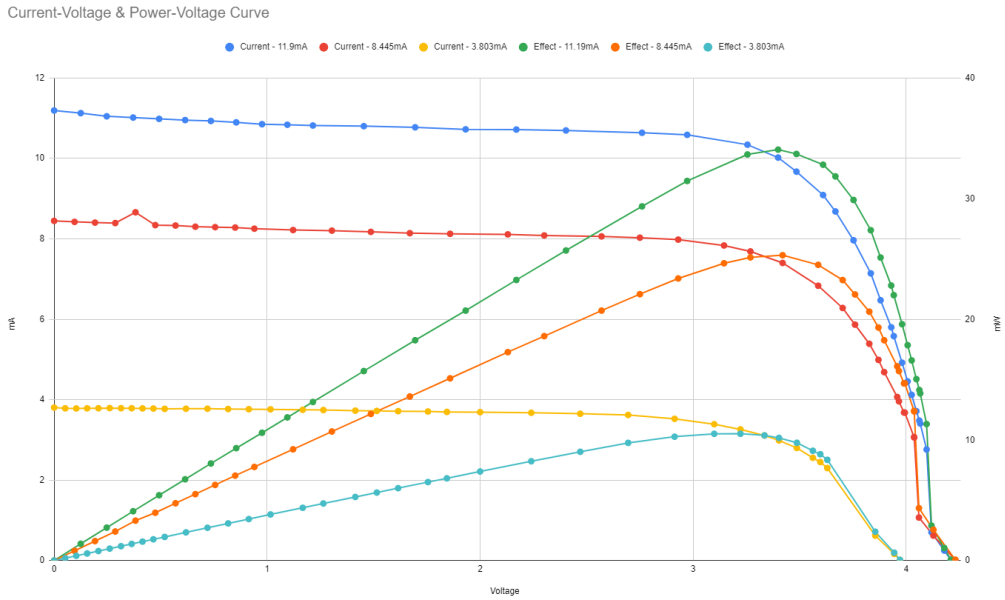


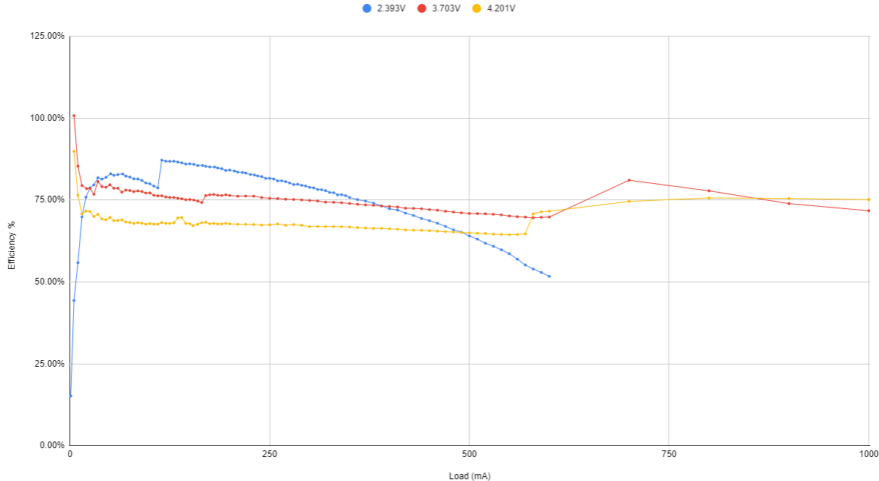
**Figure 5.1:** Power-voltage curve of the Mikroe-SW0.4M solar panel.

gives even lighting. This should be kept in mind when processing measurements from a tilted panel.

In the general usecase the PV panel will be connected to an energy harvester. A version of the power module implementation described in section 4.1.3 was realized. Its main functionality of battery charging, energy storage multiplexing, and output voltage regulation was verified to be working. In order to measure battery charging, an ammeter was connected in series with the battery at the PCB battery connector. With load disconnected, a current toward the battery was observed, using a DM-441B multimeter. Next, the multiplexing feature was tested by disconnecting either the primary or secondary battery. During disconnection, no transients in output voltage were present.

The output from the selected battery is passed to the DC-DC converter. A test was performed in order to check the general efficiency of the conversion. The adjustable HP 6652A constant voltage supply was connected to the input of the DC-DC converter through an ammeter. The IT81512A electronic load in constant current configuration is connected to the output. By varying the input voltage and output load current, the graph in figure 5.2 was made. The efficiency was calculated by division of output over input power. The measurement was performed over a wide range of currents, which required the multimeter to switch measurement ranges. This is visible in the graph as sudden jumps. In addition, the digital load is not well suited for very low currents, as it is intended for higher power use.

Efficiency vs Load Current

**Figure 5.2:** DC-DC module test.

The converter operates in two different modes, either stepping up the voltage (boost) or stepping it down (buck). These modes have different characteristics. Since the output voltage is configured to 3.3V, in figure 5.2 the 2.393V is being boosted, while the other two input voltages are being stepped down. We can observe the following trends:

- Step down conversion has best efficiency for lighter loads
- Step up conversion has best efficiency for medium loads

In the case of the step up conversion, it was also observed that for higher loads ( $>0.5A$ ) the temperature started to increase. This caused the efficiency to drop further, triggering a form of thermal runaway effect. As this is highly undesirable in a battery powered system, prolonged high current draw should be avoided. The test was performed without the power saving mode of the DC-DC converter enabled. While idle, the converter would have a constant draw of 5mA from the input source. Power saving mode should be tested to minimize this, however this signal was not made available on the prototype PCB, and was added in a later revision.

The monthly average solar radiation in the Trøndelag region is roughly 100 - 150  $Wh/m^2$  per day in January and 4000 - 5000  $Wh/m^2$  per day in July [40]. Considering the panel used in this project has a 0.4W production at an irradiance of  $1000W/m^2$ , it follows that it can extract  $400\mu W$  per  $W/m^2$ . Thus, in January, the daily power production would be about 0.05Wh, and 1.8Wh in July. Even if assuming a power module efficiency of 100%, at 3.3V this allows for an average current drain of approximately 0.63mA during January, and 22mA during July. This is a very strict power budget considering the power requirement for the wireless modem. For example, the NB-IoT has a minimal current consumption of 45mA when transmitting [13]. This also means that the requirement to be

able so send at maximum once per minute cannot always be achieved. A larger panel is therefore desirable. As long as the voltage of a larger panel does not exceed 5.5V, the same energy harvester circuit can be used.

In order to measure the short circuit current of the solar panel we use an operational amplifier over a current shunt. Together with the reading from a temperature sensor attached to the solar panel, equation 3.1 can be used to find the irradiance received by the panel. Measuring the current requires that the solar panel is shorted, which will interrupt power harvesting for the duration of the sample. A potential weakness is that the energy harvester periodically measures the open circuit voltage of the PV panel at a typical 16 second interval [33]. This is used to guide the MPPT of the circuit. Should this coincide with a short circuit measurement, the power harvesting could be affected for a longer duration.

In practice, this sensor measures solar irradiance by converting short circuit current and temperature of the solar panel as in equation 3.1. Using the PV panel efficiency properties, an estimate for potential energy production can be made. However, this is an indirect method, and not all properties are known without calibration. In particular, the panel used here has an unknown temperature coefficient. More direct methods of measuring potential power, such as MPPT based sensors, could be used instead.

While the firmware for the sensor node was not completed, the nRF9160 development kit was used to test sending and receiving messages to an MQTT broker. For this, a server with CentOS operating system was used with an instance of the "ThingsBoard" software, which served as a quick solution for visualizing IoT telemetry data. Messages were sent using both a binary format, and a JSON format. While both message structures function to specification, the binary format added extra complexity at the server side.

In order to reduce required data transmission, combining and averaging sensor samples or bulk transfers should be considered. The specification in section 3.1 does not consider the need for this. In addition, due to the overhead with establishing the connection to the server, power and data can potentially be saved by keeping the device connected between sample transmissions, especially when sending frequently.

## Chapter

# 6

# Conclusion

In this project we have looked at the technical details of implementing a remote node for measuring the potential solar panel production at an outdoor location. The node is intended to operate years at a time without requiring maintenance. This introduces a number of challenges, related to power management, wireless connectivity, and instrumentation.

A short specification was made to serve as design guidelines. Both NB-IoT and LoRa LPWAN technologies are of interest as a basis for long range low power communication. The features of the device were divided into a set of modules. Then, selections of components were suggested for two separate designs, one based on a LoRa modem and one using NB-IoT. Since the two designs have the same purpose, they have a large degree of component overlap.

In order to power the device for longer periods of time, a prototype for a solar panel energy harvester was made. Since the presence of sunlight varies throughout the day, a chargeable battery was added as part of the power harvester. The power supply is able to provide a stable voltage for the system to run. However, it was discovered that the solar panel used in this project is undersized, in particular, it will not be able to support the system during the dark winter season.

In order to measure the available solar power, a sensor was designed that could leverage the solar panel already present as part of the device. Based on the short circuit current and temperature of the PV panel, solar irradiance can be calculated. However, this requires a knowledge of the panel characteristics, not all of which were available from the panel datasheet. As the measurement requires shorting out the panel, it could potentially affect the MPPT of the energy harvester in a negative manner.

A communication test using NB-IoT with MQTT was performed, and two way communication was achieved. The messages were chosen to be encoded in JSON format, which is user and prototype friendly, but is not optimal for a compact data representation. Moreover,

sending messages with a small payload is considered ineffective due to the large overhead of underlying TCP/IP connection. Finding an optimal strategy for message structure and transmission frequency should be investigated, as it significantly impacts the system performance.

The work presented in this project serves as a basis for further developing a fully functioning sensor node. Further work is discussed in section 7.

# Future Work

Based on the discussion in section 5, a number of points for future work have been identified. The implementation was not finalized, as the system remains as a collection of modules. The next step would be to assemble the proposed components in a single enclosure, and to complete the device firmware. Further, it was revealed that the power harvesting should be improved to provide a more relaxed power budget.

With a finished module, use cases of the sensor data can be further explored, in particular, how sensor data from multiple nodes can be combined. Depending on real time requirements, an optimization of the transmission strategy can be implemented. Also, a field testing of the device should be performed to gauge the device performance.

In summary:

- Combine all the separate modules on to a single PCB assembly with appropriate weather protection
- Finalize software implementation of the sensor node firmware
- Investigate optimal strategy for when to transmit data with regards to power usage
- Upgrade the power harvesting system to supply enough energy during all seasons
- Explore potential use cases for multi-node data analysis
- Field testing



# Bibliography

- [1] 94 weather Projects - Arduino Project Hub. URL <https://create.arduino.cc/projecthub/projects/tags/weather>.
- [2] Alibaba.com. URL <https://www.alibaba.com/>.
- [3] DS18B20 Datasheet. Technical report. URL [www.maximintegrated.com](http://www.maximintegrated.com).
- [4] DS3231 Extremely Accurate IC-Integrated RTC/TCXO/Crystal - Maxim. URL <https://www.maximintegrated.com/en/products/analog-real-time-clocks/DS3231.html>.
- [5] Dekningskart - Telenor, . URL <https://www.telenor.no/privat/dekningskart/#map>.
- [6] Dekningskart - Telia, . URL <https://www.telia.no/dekning/>.
- [7] IoT/M2M - Telenor Bedrift. URL <https://bedriftsbutikk.telenor.no/m2m/>.
- [8] Low power cellular IoT - nordicsemi.com. URL <http://www.nordicsemi.com/Products/Low-power-cellular-IoT>.
- [9] MAX44284 - 36V, Input Common-Mode, High-Precision, Low-Power Current-Sense Amplifier. Technical report. URL [www.maximintegrated.com](http://www.maximintegrated.com).
- [10] MPU-9250 Datasheet | TDK. URL <https://www.invensense.com/download-pdf/mpu-9250-datasheet/>.
- [11] MQTT Version 3.1.1. URL <http://docs.oasis-open.org/mqtt/mqtt/v3.1.1/errata01/os/mqtt-v3.1.1-errata01-os-complete.html>.
- [12] Monitoring and Assessing Water Quality. URL <http://www.water.wa.gov.au/water-topics/water-quality/monitoring-and-assessing-water-quality>.

- 
- [13] nRF9160 - Nordic Semiconductor. URL <https://www.nordicsemi.com/Products/Low-power-cellular-IoT/nRF9160>.
  - [14] Nasjonal frekvensplan - Frekvensportalen. URL <https://frekvens.nkom.no/#/main>.
  - [15] OASIS Advanced Message Queuing Protocol (AMQP) Version 1.0, Part 2: Transport. URL <http://docs.oasis-open.org/amqp/core/v1.0/amqp-core-transport-v1.0.html>.
  - [16] Project Sunroof data explorer: a description of methodology and inputs. Technical report. URL <https://www.google.com/get/sunroof/data-explorer/data-explorer-methodology.pdf>.
  - [17] RN2483 Advance Information. Technical report. URL <http://www.microchip.com>.
  - [18] Realtime Microseismic Avalanche Detection hookup | Projects | CircuitMaker, . URL <https://circuitmaker.com/Projects/Details/Yme-Kvistedal-2/Realtime-Microseismic-Avalanche-Detection-hookup#sectionDesignFiles>.
  - [19] Realtime Microseismic Avalanche Detection rev5B | Projects | CircuitMaker, . URL <https://workspace.circuitmaker.com/Projects/Details/Yme-Kvistedal-2/Realtime-Microseismic-Avalanche-Detection-rev5B>.
  - [20] SP-212-SS: Amplified 0-2.5 Volt Pyranometer - Apogee Instruments, Inc. URL <https://www.apogeeinstruments.com/sp-212-ss-amplified-0-2-5-volt-pyranometer/#product-tab-information>.
  - [21] SST25VF080B - Memory. URL <https://www.microchip.com/wwwproducts/en/SST25VF080B>.
  - [22] Solar Panel - alternative powering solution for your device. URL <https://www.mikroe.com/solar-panel>.
  - [23] Stop for red light – avalanche on the way! URL <https://www.ngi.no/eng/News/NGI-News/Stop-for-red-light-avalanche-on-the-way>.
  - [24] The Things Network - Map, . URL <https://www.thethingsnetwork.org/map>.
  - [25] The Working Principle of a Thermopile Pyranometer - Kipp & Zonen, . URL <https://www.kippzonen.com/News/572/The-Working-Principle-of-a-Thermopile-Pyranometer#>.
  - [26] ThingsBoard - Open-source IoT Platform. URL <https://thingsboard.io/>.
-

- 
- [27] Utfasing av 3G-nettet – hva betyr det for deg? | Telia. URL <https://www.telia.no/magasinet/utfasing-av-3g-nettet/>.
  - [28] Welcome to the nRF Connect SDK! — nRF Connect SDK 1.0.99 documentation. URL [http://developer.nordicsemi.com/nRF\\_Connect\\_SDK/doc/latest/nrf/index.html](http://developer.nordicsemi.com/nRF_Connect_SDK/doc/latest/nrf/index.html).
  - [29] What’s the Better Battery for Your Portables—Li Ion or Li Poly? URL <https://www.electronicdesign.com/power/what-s-better-battery-your-portables-li-ion-or-li-poly>.
  - [30] Zephyr Project Documentation — Zephyr Project Documentation. URL <https://docs.zephyrproject.org/latest/>.
  - [31] Specification of Li-ion Rechargeable Battery 103450AR2-1S-3M. Technical report, 2013. URL <http://www.farnell.com/datasheets/1806916.pdf>.
  - [32] TPS6120x Low Input Voltage Synchronous Boost Converter With 1.3-A Switches. Technical report, 2014. URL <http://www.ti.com/product/TPS61200>.
  - [33] bq25505 ultra low-power boost charger with battery management and autonomous power multiplexer for primary battery in energy harvester applications. Technical report, 2019. URL <http://www.ti.com/product/BQ25505>.
  - [34] R. Braden. Requirements for Internet Hosts - Communication Layers. . URL <https://tools.ietf.org/html/rfc1122>.
  - [35] R. Braden. Requirements for Internet Hosts - Application and Support. . URL <https://tools.ietf.org/html/rfc1123>.
  - [36] J. Curry and N. Harris. Powering the Environmental Internet of Things, 4 2019. ISSN 14248220.
  - [37] S. Deering and R. Hinden. Internet Protocol, Version 6 (IPv6) Specification. Technical report, 12 1998. URL <https://www.rfc-editor.org/info/rfc2460>.
  - [38] J. Dizdarević, A. Jukan, F. Carpio, and X. Masip-Bruin. A Survey of Communication Protocols for Internet of Things and Related Challenges of Fog and Cloud Computing Integration. Technical Report 1, 2019. URL <https://doi.org/0000001.0000001>.
  - [39] L. Dunn, M. Gostein, and K. Emery. Comparison of pyranometers vs. PV reference cells for evaluation of PV array performance. In *2012 38th IEEE Photovoltaic Specialists Conference*, pages 002899–002904. IEEE, 6 2012. ISBN 978-1-4673-0066-7. doi: 10.1109/PVSC.2012.6318193. URL <http://ieeexplore.ieee.org/document/6318193/>.
  - [40] D. A. Hagos, A. Gebremedhin, and B. Zethraeus. Solar Water Heating as a Potential Source for Inland Norway Energy Mix. *Journal of Renewable Energy*, 2014:1–11, 2014. ISSN 2314-4386. doi: 10.1155/2014/968320. URL <http://www.hindawi.com/journals/jre/2014/968320/>.
-

- 
- [41] A. Lyngstad, R. Braekkan, A. Moen, C. W. Stjern, and D.-I. Øien. Norges teknisk-naturvitenskapelige universitet Vitenskapsmuseet Automatiske værstasjoner og målinger av hydrologi og tele i naturreservatene Sølendet i Røros og Tågdalen i Surnadal Det skapende universitet Det skapende universitet. ISBN 978-82-7126-784-1. URL [https://www.ntnu.no/c/document\\_library/get\\_file?uuid=7be84e99-bc63-4a9e-a3d8-d4f2ea3b3002&groupId=10476](https://www.ntnu.no/c/document_library/get_file?uuid=7be84e99-bc63-4a9e-a3d8-d4f2ea3b3002&groupId=10476).
  - [42] Nexperia. PSMN1R2-30YLD N-channel 30 V, 1.2 m $\Omega$  logic level MOSFET in LFPAK56 using NextPowerS3 Technology. Technical report, 2014. URL <http://www.farnell.com/datasheets/2575346.pdf>.
  - [43] S. Patel, S. Jardosh, A. Makwana, and A. Thakkar. Publish/Subscribe Mechanism for IoT: A Survey of Event Matching Algorithms and Open Research Challenges. 2016.
  - [44] J. Postel. Internet Protocol. . URL <https://tools.ietf.org/html/rfc791>.
  - [45] J. Postel. Transmission Control Protocol. . URL <https://tools.ietf.org/html/rfc793>.
  - [46] J. Postel. User Datagram Protocol. . URL <https://tools.ietf.org/html/rfc768>.
  - [47] Rypestøl and Lars. Frekvenskompass for mobilkommunikasjon. Technical report. URL [https://www.nkom.no/teknisk/frekvens/frekvensstrategi/frekvenskompass/\\_attachment/34516?\\_ts=163d3b267b2](https://www.nkom.no/teknisk/frekvens/frekvensstrategi/frekvenskompass/_attachment/34516?_ts=163d3b267b2).
  - [48] G. Sadasivan, J. Brownlee, B. Claise, and J. Quittek. *Architecture for IP flow information export*. RFC Editor. URL <https://tools.ietf.org/html/rfc7252>.

